Time-frequency analysis for responses evoked by nociceptive and non-nociceptive stimuli based on EEG signals

Juan Pablo Lagos

2015

LUND
UNIVERSITY

Master's Thesis in
Biomedical Engineering

Faculty of Engineer LTH
Department of Biomedical Engineering

Supervisors: Frida Sandberg Ph.D
Fredy Segura Ph.D
Mario Valderrama Ph.D
Examiner: Professor. Leif Sörnmo

1

Abstract

In the pursuit of a system capable of measuring pain signals in humans we propose a method to differentiate those signals related to pain from those which are not. We performed a time-frequency analysis using the Gabor transform to have complete information about the spectrum and its behaviour through the time to study the main differences over the evoked potentials provoked by both nociceptive and somatosensory (non-nociceptive) stimulation. The setup of the experiment also allowed us to study the mismatch negativity and the differences between the potentials evoked by a deviant stimulus and the ones evoked by a standard stimulus according to the roving paradigm. The results show that nociceptive evoked potentials read over the scalp have more energy than the somatosensory evoked potentials, they also differ in the frequencies that are activated as well as the latencies where such frequencies are activated. These results were obtained after pre-processing the EEG signals mainly removing the artifacts running the independent component algorithm (ICA) which allowed us to have reliable results.

Contents

1. Abstract **3**

2. Introduction **1**

3. Background **3**

3.1 The somatic sensory system 4

3.2 Nociception 6

3.3 The EEG 7

3.4 Artifacts 11

4. Mathematical background **13**

4.1 Mathematical model for artifact contaminated EEG 13

4.2 Independent component analysis (ICA) 13

4.3 Time frequency analysis 16

5. Dataset **21**

5.1 Experimental design 21

5.2 EEG Recording 21

5.3 Definition of spatial regions of interest 22

6. Methods **24**

6.1 EEGLAB and independent component analysis (ICA) 24

6.2 Artifact rejection 32

6.3 EP's Extraction 38

6.4 Wavelet transform 39

7. Results **40**

7.1 Nociceptive active condition 41

7.2 Nociceptive passive condition 45

7.3 Somatosensory Active condition 47

7.4 Somatosensory Passive condition 50

7.5 Nociceptive vs. Somatosensory responses 52

8. Discussion **63**

9. Conclusions **65**

10. Acknowledgement **66**

Bibliography **67**

2

Introduction

Pain is an unpleasant multidimensional experience which could be largely influenced by various peripheral and cognitive factors. Therefore, the pain experience and the related brain responses exhibit high variability from time to time and from condition to condition.

The interpretation of nociceptive input ensues in the conscious experience of pain. However, pain is an unpleasant multidimensional experience, which does not simply reflect sensory information but can be substantially influence by various psycho-physiological factors. Because of a unique combination of peripheral and cognitive factors, the pain related brain responses exhibit high variability. Thus, the diagnosis and evaluation of pain still heavily rely on subjective. For these reasons, the availability of an objective assessment of pain perception that complements the subjective report would be of paramount importance in both drug discovery and clinical practice [1].

The system meant to interpret signals to determinate, in an acceptable accurate way, whether pain is present or not has not been achieved yet. However, patterns recognition applied to certain data has been an approach, potentially resulting in a related-to-pain data which could be bared in mind when inputting parameters into a complex system capable to analyse the different characteristics associated to pain and thus achieving a precise assessment for the presence of pain or even more, the level of pain experimented.

So, what could be the impact of identifying and classifying pain objectively?. From a medicine specialist stand point, getting information, about the pain being felt by a patient, that is different to that information obtained by typical written inquests or pain analog scale assessments which are based on a verbal report driven to describe the kind of pain and the location of the pain, would be very important, otherwise the assessment of pain would still be unclear.

From the patient stand point, pain is an unpleasant sensation and even when the pain plays a vital role in humans life, and in general in the animals lives, working as an instinctive alert pointing out that something is going wrong, pain could turn into a problem or a disease itself when it is about a chronic or tonic pain. Having accurate information about the pain being

experimented would give us a better diagnosis and so a better treatment for patients and likewise that would give us a great tool when treating patients who are not able to communicate efficiently and therefore not able to communicate that they're feeling pain or what the characteristics of such pain are.

The purpose of this work is to describe related-to-pain responses by performing a time-frequency analysis over EEG signals evoked by nociceptive stimulation. To do so, this document is going to be presenting a background with content discussing the somatosensory system and nociception, as well as general knowledge about the electroencephalogram and signal processing, followed by a mathematical background, the presentation of the data used for this work and the methods applied. Finally we will present the results obtained and discuss about the main findings.

3

Background

The brain processes sensorial information, controls and coordinates the movement and behaviour and also can prioritize homoeostatic corporal functions, such as heart-beats, blood pressure, fluids balance and corporal temperature. The brain is responsible of the cognition, emotions, memory and learning [2]. The brain is in charge not only of specific tasks as for example controlling the heart beat, but also of the functional integration of such tasks that can make the whole body work. It is well known that the brain is a very complex network and the information can be efficiently transmitted and processed within either the whole brain or local brain areas [3]. This complexity makes the brain a mystery and an interesting subject of study.

We can capture electric signals from the brain using the electroencephalogram, and that allows us to gather information about the brain's behaviour in either a regular or a pathologic condition. Certainly it has been applied for studying neurological disorders like epilepsy which is characterized by the frequent crisis. It would be helpful and life quality improving for patients suffering from this disease to have a system capable of predicting such crisis. As a matter of fact studying the signals obtained by the electroencephalogram (EEG) has been an approach to the anticipation of such events [4].

The EEG signals are naturally a potential difference between two points in the scalp. However such potential difference has its origin in the action potentials occurred after the synaptic transmission and finally captured by the measurement instrument which is an electrode placed in the scalp. This electrode captures the activity occurring nearby which is merely the one produced by the pyramid cells of the cerebral cortices. Several electrodes can be used at the same time in order to obtain information from different regions in the scalp for the same period of time and thus we can characterize the activity produced over one region and compare it to other regions. There are different types of electrodes but the surface or extra-cranial electrodes are the most used since they are located in the scalp and represent a non-invasive method. However they might have a delay in the electric signal and a minor amplitude [5].

Using several electrodes to record brain activity is certainly useful when we try to record a large number of cortical neurons simultaneously but also represents a challenge in terms of how to analyse and correlate such a big data. In a study made in the University of Fudan for example, multi-neuronal activity of multi-electrode recordings in the prefrontal cortex was analysed for a rat during a Y-maze working memory task and this way describing the small-world properties and the functional networks [3].

Pain may be very well defined as a personal experience that can be affected by several factors. Thus the brain response to pain-related stimuli may vary from person to person and time to time and also according to the condition on how pain is presented. This is what would make an objective assessment of pain a great breakthrough for basic and clinical applications [1].

Everybody have this kind of sensation because the pain is a natural warning for react in order to protect a whole body. However, the reaction from the pain sometimes have to be avoided because the overreaction causes some damages to near-by tissue [6], due mainly to the brain responses which lead to a disconnection of the generation of pain by the initial tissue injury, and consequently loss of responsiveness to treatment that can overcome the pain [7]. Therefore, the system that can indicate pain level needs to be achieved.

Different algorithms for treating EEG data have been tried in order to estimate the presence of pain and the pain level. One of them has been the fuzzy logic algorithm combined with the kernel support vector machine (SVM) [6]. The subjective and uncertainty nature of pain justifies the use of fuzzy logic and then the use of the kernel support vector machine (SVM) helps to create a linear line to separate the data in pain state or non-pain state. This method has proved to be suitable for the classification of pain.

The brain has always been an enigma for the human being. Tools of every kind have been developed to analyse and comprehend the brain. Thus it has been studied from different perspectives like medicine, psychiatry, psychology, biology and others like engineering.

However, if recording the brain activity represents a challenge itself, trying to recognize patterns and extracting the main features from the brain ativity is even more challenging. Therefore mathematical models have been developed in order for us to be able to apply algorithms that allow us to go through the brain signals in an manner that can provide us of reliable results.

3.1 The somatic sensory system

The somatic sensory system is considered to be one of the most complex systems in the human body, it is in charge of a wide range of sensations that vary from touch-sense, pressure, vibration, limb position, heat, cold, and pain. Such sensations are triggered by different events and captured by specialized

receptors contained mostly in the skin and muscles. The information travels all the way from the receptors to the central nervous system. The whole nervous system is also divided into subsystems functionally different and with different receptors and pathways [8]. There are basically three types of subsystems, one in charge of transmitting painful stimuli and changes in temperature, another in charge of transmitting stimuli originated from cutaneous level such as vibrations or touches and pressure, and one third subsystem related to muscles, tendons and joints, which is in charge of the sensing the position of the body parts in space.

When it comes to a somatic sensation, it is originated from the activation of afferent nerve fibers which extend to the skin and muscles where the action potentials are the first product of the stimulation. The information is passed to the location of the cell body in the ganglia and then it propagates to the synaptic terminals of the fibers located in the central nervous system. The pass of the information through the body cell is not a mandatory step, however cell bodies play a vital role in maintaining the cellular machinery that mediates transduction, conduction, and transmission by sensory afferent fibers.

The transduction of the energy of one stimulus into an electrical signal pass across the body is ruled by the same principle for all somatic sensory afferents: first a stimulus changes the permeability of the cation channels in the endings of the afferent nerve, thus it generates a depolarizing current or what is called a receptor potential. In the afferent fibers, the action potential is only generated if the receptor potentials is large enough to reach the threshold. When the threshold is reached, the action potential generated is proportional to the magnitude of the receptor potential.

There are two types of afferent fibers, the ones that are encapsulated by specialized receptor cells and the ones which are not. The once without any encapsulation are related to the sensation of pain, and are known as free nerve endings fibers. On the other hands the afferent fibers which do have encapsulation are more related to eliciting somatic sensations not necessarily related to pain and are characterized by a low threshold for action potential. Besides, other characteristics like the size of the diameter of the fibers make differ the sensory afferents from each other, and depending on the diameter the functionality of the afferents also change. The largest diameter sensory afferents are known as Ia and they provide the sensory receptors in the muscles. Smaller diameter fibers ($A\beta$ afferents) are mostly related to handle the information provoked by touch and even smaller diameter fibers ($A\delta$ and C) receive and transmit the information about pain and change in temperature. Also the size of the receptive field area of the skin surface over which stimulation results in a significant change in the magnitude of the action potentials. The receptive fields in regions with dense innervation like fingers, lips and toes, are smaller than those in the forearm or back whose density of afferent

fibers is smaller [8].

Thus the transmission of information start with the action potentials generated by different types of receptors and then the information is passed to the central nervous system through a chain of neurons which are classified in three different groups. The ones located in the dorsal root an cranial nerve ganglia, the ones located in the brain-stem nuclei and the ones in the thalamus from where the information is projected to the cerebral cortex [9].

3.2 Nociception

Nociception is referred to as a the perception of pain. It is also related to the system in charge of alerting the brain that the body is physically in danger when any noxious stimulus occurs. Although the transmission of nociceptive information is similar to the transmission of somatic non-nociceptive information, these two differ in the type of receptors and the pathways. There is still a lot to be discovered on how the brain manages the information related to pain and that is why this is a big area of research.

The cells that initiate the sensation of pain are called nociceptors. Their mechanism to transduce stimuli into a receptor potential is the same as the one described for the somatic non-nociceptive case. The nociceptors also arise from cell bodies in the dorsal ganglia that send one axonal process to the periphery and other process inot the brain-stem.

The axons related with nociceptors have a relatively slow conduction velocity. These axons which transmit the information associated with pain might be classified either within the $A\delta$ group of afferent which conduct at 5-30 m/s or within the C fiber group which conduct at even smaller velocities usually less than 2 m/s. The $A\delta$ nociceptors respond to dangerously mechanical and thermal stimuli, on the other hand the C nociceptors respond mechanical, chemical and thermal stimul, these are known as polymodal nociceptors.

The way how human body perceives pain is still a field being studied, and some experiments have been made with volunteers who are submitted to pain stimulation, and frequently the participants are asked to rate the pain experimented as well as describe the sensations elicited by the stimulation. In general pain has been classified in two groups, one where pain is perceived as a sharp painful sensation and the other where pain is perceived as a diffused and long-lasting sensation [8].

A distinct set of pain afferents with membrane receptors known as nociceptors transduces noxious stimulation and conveys this information to neurons in the dorsal horn of the spinal cord. The major central pathway responsible for transmitting the discriminative aspects of pain (location, intensity and quality) differs from the mechanosensory pathway primarily in that the central axons of dorsal root ganglion cells synapse on second-order neurons in

the dorsal horn; the axons of the second-order neurons then cross the midline in the spinal cord and ascend to thalamic nuclei that relay information to the somatic sensory cortex of the postcentral gyrus. Additional pathways involving a number of centers in the brainstem, thalamus, and cortex mediate the affective and motivational responses to painful stimuli. Descending pathways interact with local circuits in the spinal cord to regulate the transmission of nociceptive signals to higher centers [9].

3.3 The EEG

Electric and magnetic fields are found mainly in the cerebral cortex, these are the result of several electrical signals generated from the flow of ions when the neurons respond to different stimuli. The cerebral cortex contains around 10^9 to 10^{10} neurons [10] and we can measure the electrical activity resulted from a summated electrical signals driven by these cells in order for us to be able to describe how brain works. Such electrical activity can be captured by electrodes placed in the scalp, however amplification is required since the order of the signal at scalp level is just hundreds of mV or less. This electrical activity recorded is known as electroencephalogram or simply the EEG.

The electrodes used to record the electrical activity of the brain are usually placed following a standard system. Such system is related to the anatomical structures of the brain like for example frontal, temporal or occipital. The electrical activity is also related to this anatomical structures and it means that the electrical activity is not uniformly distributed on the scalp.

The electrical activity measured from scalp is not randomly produced in the sense that it responds to specific events. The EEG is a noninvasive tool very useful to characterize the oscillatory signals from the brain. EEG has also brought important breakthroughs and many applications have been created in the field of clinical neurophysiology, and some interfaces have been designed to enhance the communication and control abilities of motor-disabled people [11]. Also EEG is used to monitor the state of the neurological brain, and thus detecting any disorder or cerebral damage that might be present.

However since the brain responds to several stimuli at the same time, it is no that easy to obtain a significant result after using the EEG. So in order to obtain statistically significant results, exhaustive analysis are required before making any conclusion. The main issues to deal with when using EEG could be enclosed as follows:

1. Placement of the scalp electrodes and the data acquisition,
2. Variability of the brain wave patterns,
3. Scalability to a larger population,
4. Heritability of the EEG patterns.

The EEG is basically fed by millions of neurons with similar spatial ori-

entation and whose activity is detected from scalp. The number of electrodes used to record the electrical activity can vary from 19 to 256 depending on the spatial resolution needed. However it is necessary to be very careful because an inappropriate spatial separation of the electrodes might cause distortion to the estimated potential on the scalp. Also a reference electrode is needed so the potentials recorded from other electrodes can be measured with respect to the reference channel or electrode. A bad reference could lead to bad interpretation of the brain waves [12].

An EEG is characterized by small amplitude (μV) noisy signal that ranges from 0.5 to 30-40Hz [13]. At this point it is important to mention that when working with EEG one will have to deal with artifacts, most of them are generated from the body itself mainly caused by eye blinking, eye movements, muscle activation and muscle activation. On the other hand a bad placement of the electrodes can cause the electrodes to pop out or even a slight movement of them might cause noise in the signal, also a bad grounding of the electrodes could result in a strong signal over the 50Hz and 60Hz frequencies associated with the power lines. For all of these reasons, acquiring EEG data has to be done under the proper conditions in order to obtain significant results.

Another feature of the brain waves is the dependency on the brain state. It means that the results may vary depending on whether the subject is sleeping, thinking, relaxed, walking or visualizing something. In order to obtain a statistically significant result one would have to have the maximum control possible of these variables. Besides the brain responses also change according to the age, the EEG in childhood for example shows slower frequency oscillations than an adult [12].

The 10/20 system

The 10/20 system describes standard locations for the electrodes used in the EEG. This system is largely and internationally recognized and accepted.

The system was created bearing in mind two criteria, the location of the electrode itself and the underlying area of the cerebral cortex. The distances between the closest electrodes are either 10% or 20% of the total front-back orright-left distance of the skull and that is why this system is known as the "10/20 system". Each electrode is given a letter and a number, the letter let us identify the lobe and the number depends on the hemisphere, even numbers refer to electrode positions on the right hemisphere and odd numbers refer to electrode positions on the left hemisphere. The letters "C" and "z" are used only for identification purposes since there are not such a "C lobe" or "z lobe".

Four anatomical landmarks are used for the essential positioning of electrodes: first, the nasion which is the point between the forehead and the nose; second, the inion which is the lowest point of the skull from the back of the head and is normally indicated by a prominent bump; the pre auricular points

Electrode	Lobe
F	Frontal
T	Temporal
C	Central *
P	Parietal
O	Occipital

Table 3.1: Electrodes labels.

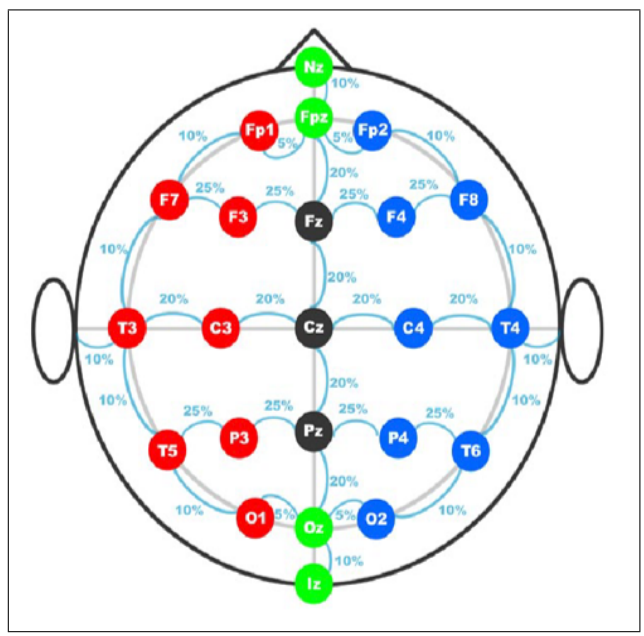

Figure 3.1: 10/20 system.

anterior to the ear. Also extra positions can be added by utilizing the spaces in between the existing 10/20 system [14].

Electrical activity measured from scalp

The electrical activity from one neuron is not measurable with EEG due to the different layers such as tissue or skin that attenuate the signal but the activity resulted from summation of millions of neurons is actually measurable from scalp and the more neurons presenting synchronized activity the larger the EEG signal will be, because the electric field produced by individual neurons will add up. Likewise, if the activity from individual neurons is asynchronous, the EEG signal will be a characterized by a low amplitude waveform. When the synchronous activity is repeated continuously then the result will be an rhythmic EEG. Such activity is produced from many millimeters depth and it is strong enough to be detected by an electrode placed in the scalp. Sometimes this collective electrical activity presents a repetitive and oscillatory behavior , this is usually called a rhythm. The electrode then, detects these rhythms generated by the currents originated during the synaptic excitation of the dendrites.

The EEG rhythms basically depend on the mental state of the subject, and the rhythm obtained during a sleeping state of the brain is way different from the rhythm obtained during a state of attention or attentiveness. These rhythms in general are characterized by their frequency and amplitude. The frequency of an EEG rhythm is sustained by activity coming from the thalamus, in which the neurons have the ability to generated a constant and sustained rhythmic pattern. Some rhythms are also generated by the interactions between neurons found in the cortex. In general high frequency rhythm is associated with alertness or dream sleep, in contrast, the low frequency rhythms are related to drowsiness and non-dreaming sleep states [13].

Brain natural frequency bands

EEG signals are characterized by amplitudes between few microvolts to approximately 100 μV, although some perturbations may introduce some noise even larger. The frequency of EEG signals are basically within the range of 0.5 to 30-40 Hz. This range is divided in five groups or frequency bands for which some brain states make them dominate some regions in the scalp. For these frequency bands the brain states related to them have been described [13]:

Delta rhythm: $<$4 Hz. These frequencies are found during deep sleep state of the brain and such signals are characterized by a large amplitude.

Theta rhythm: 4-7 Hz. The theta rhythm is related to drowsiness and in certain stages of sleep.

Alpha rhythm: 8-13 Hz. Alpha rhythms are mostly presented in subjects who are awake with eyes closed. Occipital regions are characterized by a larger

amplitude when this rhythm is present.

Beta rhythm: 14-30 Hz. This rhythm is also present during some sleep stages and is mostly present in the frontal and central regions of the scalp.

Gamma rhythm: >30 Hz. Gamma rhythm is associated with states of alert and active information processing of the cortex.

Evoked potentials

The electrical response of the brain to different types of stimuli like auditory, visual or painful stimulation is referred to as "Evoked potential" and it is described as an event-related activity. The extraction of such potentials gives access to valuable information such as location of brain lesions, sesory pathways abnormalities and other types of disorders. Different types of stimuli lead to different types of evoked potentials, so the characteristics of these potentials like the amplitude or spectrum may differ from each other depending on the event that triggered the electrical response in the brain-stem. Furthermore, once again the state of the brain also affects the morphology of the evoked potentials [13].

Even though the EEG signal ranges up to 100 μV, the evoked potentials are characterized for ranging from 0.1 to 10 μV. According to this, the noise is indeed an important issue to deal with since the evoked potentials represent such small magnitude signals. However the evoked potentials are usually related to a certain event, it means that most of the times we expect to find the evoked potentials within some period of time after the stimulus [13].

3.4 Artifacts

When it comes to electrical signals measurement, it is usual to have noise and artifacts that we would like to reject from our data. EEG signals are not an exception and it is common to have several noise sources contaminating the data whilst it is being measured. In order to have reliable results from EEG data analysis it is crucial to deal with the noise sources and reject them as far as we can.

In EEG signals, the artifacts often come as high amplitude signals if compared to those naturally evoked by brain activity and even though they might be uniformly distributed across the data they could bias evoked potential or other averages constructed from the data and consequently we could infer wrong breakthroughs after data analysis.

Artifact processing has become more and more a relevant issue to deal with in order to obtain significant results. EEG artifacts are mainly produced by physiological and technical origins [13]:

Eye movement and blinks: The electrical activity produced by eye movement is referred to as electrooculogram (EEG) signals. This signals are

usually strong and are detecting by the EEG, however it varies depending on the proximity with electrode and direction in which the eyes are moving.

Muscle activity: The muscles movement can introduce a perturbation in the EEG signal. The electrical activity of the muscles is measured on the body surface using electromyograph (EMG). Depending on how hard is the muscle contraction the EEG signal will present strong or weak spikes in the EEG signal, the harder the contraction is the larger of the spikes, also the time between the spikes will decrease as the contraction strength increases.

Cardiac activity: The electrical activity of the heart can also be reflected in the EEG. Nevertheless this activity is much smaller on the scalp compared to the EEG signals with different origin.

Electrodes and equipment: A bad placement of the electrodes may cause them to move or if the electrode-scalp contact is not good it produces an artifact known as electrode-pop and it is characterized by a change in the baseline level which usually returns to the original one. Furthermore if the electrodes are not shielded enough, the 50/60 Hz signals coming from the power lines will be reflected in the EEG as a constant signal over these frequencies.

4

Mathematical background

4.1 Mathematical model for artifact contaminated EEG

One could think of the EEG as a signal composed by two signals, one which is the noise $v(n)$ and the other one coming from the cerebral activity $s(n)$. If the EEG is the result of the sum of these two signals ($v(n)$ and $s(n)$), we could estimate the noise $v(n)$ and the subtract it from the observed signal $x(n)$ and thus we would be cleaning the EEG data [13],

$$x(n) = s(n) + v(n) \tag{4.1}$$

This is associated with subtracting methods and also underlines noise reduction through linear filtering, this case applied to x(n). This model is known as the additive model, it is simple and easy to handle, and several methods have been developed for optimal estimation of $s(n)$. However other models have been proposed, and certainly they might be more suitable. In eq. (4.2) is shown the multiplicative method in which the signal $s(n)$ and the noise $v(n)$ interact in a multiplicative way:

$$x(n) = s(n)v(n) \tag{4.2}$$

The solution for separating the signals $s(n)$ and $v(n)$ were developed in 1960's and yet have received marginal attention [13]. However, this model will be suitable for the artifact rejection used in this work as we are going to explain later in this section.

4.2 Independent component analysis (ICA)

A big challenge in neural network research, is finding a model or a suitable representation of multivariate data. Treating the data as linear combination of the original variables has brought simpler concept and a much easier solution for computational interfaces. Independent component analysis (ICA)

is a method in which it is attempted to fin a linear representation of non-Gaussian data so that the components are statistically independent, or at least as independent as possible. This representation of the data has helped to the feature extraction and signal separation [15].

If we think of the EEG signals as a result of the summation of different sources, in which are included both the artifacts and the features in which we do have certain interest, we could then attempt to remove the artifacts from the sample data by identifying the independent components or sources that are related to such artifacts and thus from that point we could perform signal processing based on data that after having run the ICA and removing the right sources is almost free of artifacts.

However, removing the right sources supposes a challenge and it is even more complex than running the ICA algorithm itself. The components may either be classified as artifact related sources or not and the criteria for doing so is related to the properties of the component itself. The challenge relies on the fact that such properties might have some variations from time to time and across subjects, so in order to outcome this challenge it is necessary to look carefully at the features and characteristics of every component to make a good approximation.

One of the mos basic methods for dealing with artifacts in EEG data is the one based on the detection of out-of-bounds potentials. Once given the parameters of the maximum and minimum amplitudes in the signals, a threshold is defined and the data out of this limits is simply rejected. However this simple method might not detect the artifacts whose amplitude is small enough to be within the limits of rejection, for example most of the artifacts related to muscle movement are usually small as well as some small eye movement artifacts.

The independent component analysis (ICA) has proven to be an efficient method for detecting artifacts and separating artifactual processes. ICA is actually considered an important technique for removing artifacts [16].

Independent Component Analysis, as the name implies, can be defined as the method of decomposing a set of multivariate data into its underlying statistically independent components. In this model, we observe n random variables $x_1(t), x_2(t), ..., x_n(t)$, associated to n number of EEG channels or electrodes, which are linear combinations of n random latent variables $u_1(t), u_2(t), ..., u_n(t)$ as:

$$x_i(t) = a_{i1}u_1(t) + a_{i2}u_2(t) + ... + a_{in}u_n(t) \; \forall \; i = 1, ..., n \tag{4.3}$$

Where $a_{ij}, \text{for} j = 1, ..., n$ are some real coefficients. By definition, the sources u_i are statistically independent. The "latent variables" are the sources $u_i(t)$, which are referred to as independent components. They are called "latent" because they cannot directly be observed. Both the independent components, $u_i(t)$, and the mixing coefficients, a_{ij}, are not known and must

be determined using only the random variables $x_i(t)$. The ICA latent variables model is better understandable if it is presented in matrix form. If $U = [u_1(t), u_2(t), ..., u_n(t)]^T$ represents the original multivariate data that is transformed through some transformation matrix H producing X such that:

$$X = HU \tag{4.4}$$

Then ICA tries to identify an unmixing matrix W such that:

$$W = H^{-1} \tag{4.5}$$

So that the resulting matrix Y is:

$$Y = WX = W(HU) = U^{'} = U \text{ (since } W = H^{-1}) \tag{4.6}$$

The ICA demands that the original signals $u_1(t), u_2(t), ..., u_n(t)$ be at any time instant t statistically independent and the mixing of the sources be linear [17].

Secondly, the number of mixtures must be equal to the number of sources and the mixtures must be linearly independent from each other. Third, the only source of stochasticity in the model is U. The model must be thus be noise free. Fourth, it is assumed that the data are centered (zero mean). Also for some algorithms, the data must be pre-processed further. Fifth, the source signals must not have a Gaussian probability density function (pdf) except for one single source that can be Gaussian [18].

Statistical independence

Let $x_1(t), x_2(t), ..., x_n(t)$ random variables with pdf $f(x_1(t), x_2(t), ..., x_n(t))$, then the variables $x_i(t)$ are mutually independent if:

$$f(x_1(t), x_2(t), .., x_n(t)) = f_1(x_1(t))f_2(x_2(t))...f_n(x_n(t)) \tag{4.7}$$

That is, if the pdf of the $x_i(t)$ is equal to the multiplication of each marginal pdf of the $x_i(t)$. Statistical independence is a more severe criterion than uncorrelatedness between two variables. If we take random centered variables, uncorrelatedness is expressed by the following equation:

$$E[x_i(t)x_j(t)] - E[x_i(t)]E[x_j(t)] = 0 \text{ for } i \neq j \tag{4.8}$$

Where $E[.]$ is the expectation. On the other hand, independence can be defined using the expectation by the following:

$$E[g_1(x_i(t))g_2(x_j(t))] - E[g_1(x_i(t))]E[g_2(x_j(t))] = 0 \text{ for } i \neq j \tag{4.9}$$

For all functions g_1 and g_2. In the particular case where the joint pdf of the variables is Gaussian, uncorrelatedness is equivalent to independence.

There are several ways to measure independence and each of them involves the use of different algorithms when it comes to perform an ICA, which results in slightly different matrices [18].

Minimization of mutual information

Mutual information is defined for a pair of random variables as:

$$I(X;Y) = H(X) - H(X|Y) \tag{4.10}$$

Where $H(X|Y)$ is the conditional entropy and H(X) is the entropy of X. Conditional entropy is given by:

$$H(X|Y) = H(X,Y) - H(Y) \tag{4.11}$$

Where H(X,Y) is the joint entropy of X and Y and $H(Y)$ is the entropy of Y. Therefore, going back to the eq. (3.10), mutual information can be seen as the reduction of uncertainty regarding variable X after the observation of Y. Consequently if we had an algorithm to minimize mutual information, we would be searching for the components u_i that are maximally independent [18].

InfoMax algorithm

Using Equation 3.10 and after some manipulation. Amari et al. (1996) proposed the following algorithm to compute the unmixing matrix W (called InfoMax) [18]:

1. Initialize $W(0)$ (e.g. random)
2. $W(t+1) = W(t) + \eta(t)(I - f(Y)Y^T)W(t)$
3. If not converged, go back to step 2

Where t represents a given approximation step, $\eta(t)$ a general function that specifies the size of the steps for the unmixing matrix updates (usually an exponential function or a constant), $f(Y)$ a nonlinear function usually according to the type of distribution (super of sub-Gaussian), I the identity matrix of dimensions mxm and T the transpose operator. In the case of super-Gaussian distribution, $f(Y)$ is usually set to:

$$f(Y) = \tanh(Y) \tag{4.12}$$

And for sub-Gaussian distribution, $f(Y)$ is set to:

$$f(Y) = Y - \tanh(Y) \tag{4.13}$$

4.3 Time frequency analysis

One could think of the Fourier transform as a method to extract the spectral information from the signal, and indeed is a good and recommended method. However to obtain full knowledge of the signal you must perform a time-domain analysis as well. The Fourier transform, despite of being a good approach, is not adequate specially for procedures associated with analysis of

non-stationary signals and real-time processing. D. Gabor might be the first person to make the observation about the deficiency of the formula of the Fourier transform, arguing that information about the spectral information over the time is not presented in the results of the Fourier transform. Indeed, in the extreme case, the Fourier transform of the delta distribution $\delta(t - to)$, with support at a single point t_0 is $e^{it_0 w}$, which certainly covers the whole frequency domain.

D. Gabor introduced a time-localization "window function" $g(t-b)$, where the parameter b is used to translate the window in order to cover the whole time-domain, for extracting local information of the Fourier transform of the signal. A Gaussian function would be chosen by Gabor as the one suitable for the window function g.

The Gabor transform

Given a function $f(t)$ in $L^2(\Re)$ with finite energy and representing an analog signal, its Fourier transform is defined by eq. (4.14).

$$\hat{f}(w) = \int_{-\infty}^{\infty} e^{-iwt} f(t) dt \tag{4.14}$$

By computing eq. (4.14) we obtain information of the spectral aspect of the signal $f(t)$. However if we wanted to extract information of the spectrum $\hat{f}(w)$ from local observation of the signal $f(t)$ we would need a time-window function. Such time-window for time-localization is achieved by using a Gaussian function and the width of the window is determined by a fixed positive constant α. We can use a Gaussian function as the one presented in eq. (4.2)

$$g_\alpha(t) := \frac{1}{2\sqrt{\pi\alpha}} e^{-\frac{t^2}{4\alpha}} \tag{4.15}$$

where $\alpha > 0$ is fixed. For any value of $\alpha > 0$, the Gabor transform of an $f(t) \in L^2(\Re)$ is defined by

$$(G_b^\alpha f)(w) = \int_{-\infty}^{\infty} e^{-iwt} f(t) g_\alpha(t - b) dt \tag{4.16}$$

It implies that with $(G_b^\alpha) f(w)$ we are evaluating the Fourier transform of $f(t)$ around $t - b$ given the width of the time-window which is determined by α.

If we set a function $G_{b,w}^\alpha f$ defined as follows:

$$G_{b,w}^\alpha(t) := e^{-iwt} g_\alpha(t - b) \tag{4.17}$$

then we have

$$(G_b^\alpha f)(w) = \langle f, G_{b,w}^\alpha \rangle = \int_{-\infty}^{\infty} f(t) G_{b,w}^\alpha(t) dt \tag{4.18}$$

We may interpret this expression in eq. (4.18) as windowing the function $f(t)$ by using the window function $G_{b,w}^\alpha f$ in eq. (4.17).

One advantage of the formulation in eq. (4.18) is that the Parseval Identity can be applied to relate the Gabor transform of f with the Gabor transform of $\hat{f}$. Using eq. (4.19) and eq. (4.17)

$$\hat{g}_\alpha(w) = e^{-\alpha w^2} \tag{4.19}$$

We obtain:

$$\hat{G}_{b,w}^\alpha(\eta) = e^{-ib(\eta - w)} e^{-\alpha(\eta - w)^2} \tag{4.20}$$

Now for an $\alpha = 1/4\alpha$ We have

$$\begin{aligned} G_{b,w}^\alpha(w) &= \langle f, G_{b,w}^\alpha \rangle = \frac{1}{2\pi} \langle \hat{f} \hat{G}_{b,w}^\alpha \rangle \\ &= \frac{1}{2\pi} \int_{-\infty}^{\infty} \hat{f}(\eta) e^{-ib(\eta - w)} e^{-\alpha(\eta - w)^2} d\eta \\ &= \frac{e^{-ibw}}{2\sqrt{\pi\alpha}} \int_{-\infty}^{\infty} (e^{ib\eta} \hat{f}(\eta)) g_{1/4\alpha}(\eta - w) d\eta \\ &= \frac{e^{-ibw}}{2\sqrt{\pi\alpha}} (G_w^{1/4\alpha} \hat{f})(-b) \end{aligned} \tag{4.21}$$

We interpret eq. (4.21) from two different points of view. First we consider

$$\begin{aligned} &\int_{-\infty}^{\infty} (e^{-iwt} f(t)) g_\alpha(t - b) dt \\ &= (\sqrt{\frac{\pi}{\alpha}} e^{-ibw}) \cdot \frac{1}{2\pi} \int_{-\infty}^{\infty} (e^{ib\eta} \hat{f}(\eta)) g_{1/4\alpha}(\eta - w) d\eta \end{aligned} \tag{4.22}$$

Then it turns to be that the "window Fourier transform" of $f(t)$ with window function g_α at $t = b$ is the same as the "window inverse Fourier transform" of $\hat{f}$ with the exception of the coefficient $\sqrt{\frac{\pi}{\alpha} e^{-ibw}}$

Secondly we consider:

$$H_{b,w}^\alpha(\eta) := \frac{1}{2\pi} \hat{G}_{b,w}^\alpha(\eta) = (\frac{e^{ibw}}{2\sqrt{\pi\alpha}}) e^{-ib\eta} g_{1/4\alpha}(\eta - w), \tag{4.23}$$

we have

$$\langle f, G_{b,w}^\alpha \rangle = \langle \hat{f}, H_{b,w}^\alpha \rangle \tag{4.24}$$

In conclusion, the information obtained by analyzing the signal $f(t)$ at the time point $t = b$ when using the window function $G^{\alpha}_{b,w}$ as shown in eq. (4.18) can also be obtained by analyzing the spectrum $\hat{f}(\eta)$ of the signal in a neighborhood of the frequency $\eta = w$ by using the window function $H^{\alpha}_{b,w}$ as defined in eq. (4.23).

By definition we know that the width of the time-window is two times the standard deviation of the window function. Calculating the standard deviation for the window functions we obtain:

$$\Delta_{G^{\alpha}_{b,w}} = \sqrt{\alpha} \tag{4.25}$$

and

$$\Delta_{H^{\alpha}_{b,w}} = \frac{1}{2\sqrt{\alpha}} \tag{4.26}$$

The product of the width of the time-window $G^{\alpha}_{b,w}$ and that of the frequency-window $H^{\alpha}_{b,w}$ is

$$(2\Delta_{G^{\alpha}_{b,w}})(2\Delta_{H^{\alpha}_{b,w}}) = (2\Delta_{g_{\alpha}})(2\Delta_{g_{1/4\alpha}}) = 2 \tag{4.27}$$

The cartesian product of these two windows is:

$$[b - \sqrt{\alpha}, b + \sqrt{\alpha}] \times \left[w - \frac{1}{2\sqrt{\alpha}}, w + \frac{1}{2\sqrt{\alpha}}\right] \tag{4.28}$$

This is called a rectangular time-frequency window. It is plotted in the time-frequency domain to show how a signal is localized. The width $2\sqrt{\alpha}$ of the time-window is referred to as the "width of the time-frequency window", and the width $\frac{1}{\sqrt{\alpha}}$ of the frequency window is called the "height of the time-frequency window". A plot of this window is shown in Fig. 4.1 Observe that the width of the time-frequency window is unchanged for observing the spectrum at all frequencies [19].

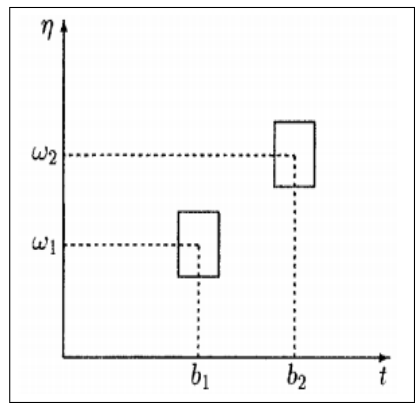

Figure 4.1: Gabor window.

Let us make an example for a signal like this [20]:

$$\begin{aligned} x(t) &= cos(\pi t) \text{when} t < 10 \\ x(t) &= cos(3\pi t) \text{when} 10 <= t < 20 \\ x(t) &= cos(2\pi t) \text{when} t >= 20 \end{aligned} \tag{4.30}$$

Then when we compute the Gabor transform we would expect a result as shown in fig. 4.2, where the grey tones represent higher power spectrum as expected given the signal $x(t)$

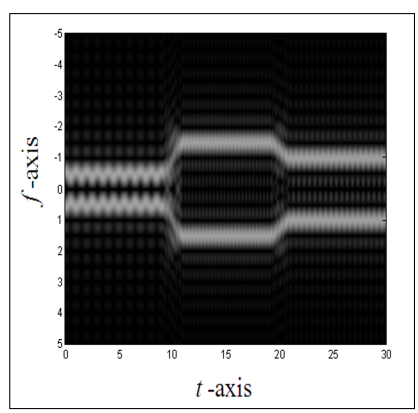

Figure 4.2: Gabor plot.

5

Dataset

The dataset used in this study comes from the same database acquired in the paper "Mismatch responses by nociceptive stimuli" [21] whose authors (Li Hu, Chen Zhao, Hong Li and Elia Valentini) obtained by experimenting and measuring EEG signals under certain parameters which will be exposed in this chapter. However we only had access to the data corresponding to 8 subjects of 16 subjects whom were experimented with in such study.

5.1 Experimental design

In [21] the event-related potentials were recorded in four sessions (two modalities: non-nociceptive somatosensory and nociceptive stimuli; two conditions: active and passive), and two repeated blocks were included in each session. Block order was counterbalanced across participants. In each block, trains of non-nociceptive somatosensory and nociceptive stimuli were delivered to lateral (L), median (M), or wrist (W) section of the participants' right and left hands, respectively. Each block had about 50 trains of stimuli with an intertrain interval of 1000ms. Each train consisted of 4-8 repeated identical stimuli delivered to the same section at a constant interstimulus interval of 1000ms. In each modality participants were required either to focus their attention on the stimuli in two blocks (A: active condition), or focus their attention on watching a silent video in the remaining two blocks (P: passive condition). The first stimulus in each train was a deviant that became standard (the last stimulus in each train) through repetition. This design provided four conditions (Ad,As,Pd,Ps). In this paradigm, deviants and standards had exactly the same number of trials and physical properties [21].

5.2 EEG Recording

The EEG recording used in [21] a Brain Products system (bandpass: 0.01 - 100Hz, sampling rate: 500Hz) was used, connected to a standard EEG cap with 60 scalp Ag - AgCl electrodes placed according to the 10-20 system. The

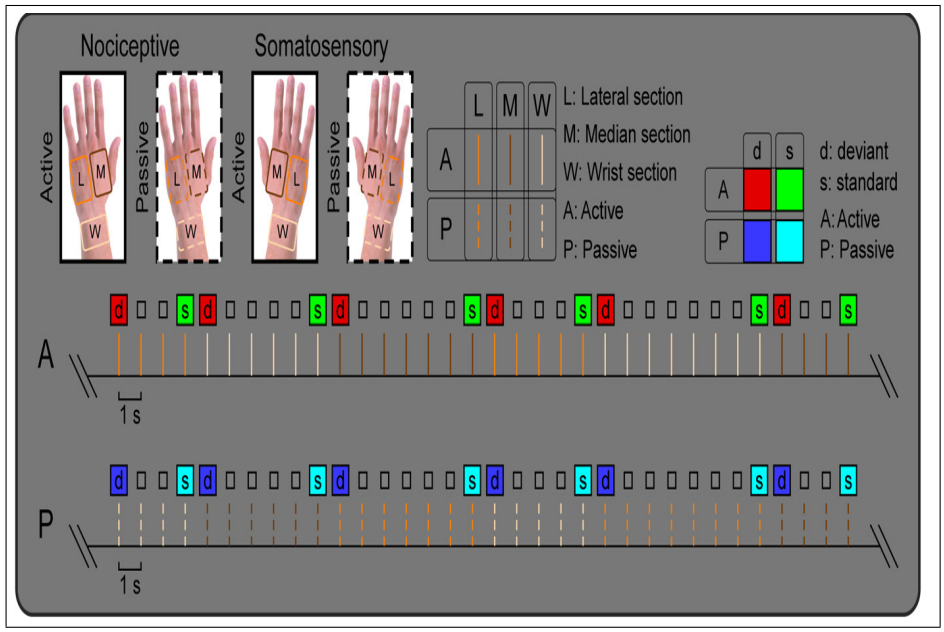

Figure 5.1: Experimental Design [21].

left mastoid was used as reference channel, and all channels impedances were kept below $5k\Omega$. To monitor ocular movement and eye blinks, electrooculographic (EOG) signals were simultaneously recorded from four surface electrodes placed on the upper and lower eyelid and next by the outer canthus of the left and right eye [21].

5.3 Definition of spatial regions of interest

A two way repeated measures ANOVA was performed in [21] in order to assess the effects of mismatch (two levels: deviant vs. standard) and attention (two levels: active vs. passive) on both somatosensory evoked potentials and nociceptive evoked potentials, to define the significant spatial regions of interest (sROI's). Consequently scalp topographies were obtained for both somatosensory and nociceptive blocks for the four experimental conditions (Ad,As,Pd,Ps) in steps of 20ms. The conditions for a sROI to be defined as significant were to be composed by at least two nearby channels and it had to be composed by more than 10 consecutive significant time points (20ms) for the factor mismatch and attention, respectively ($F > 8.9$, $p<.01$)

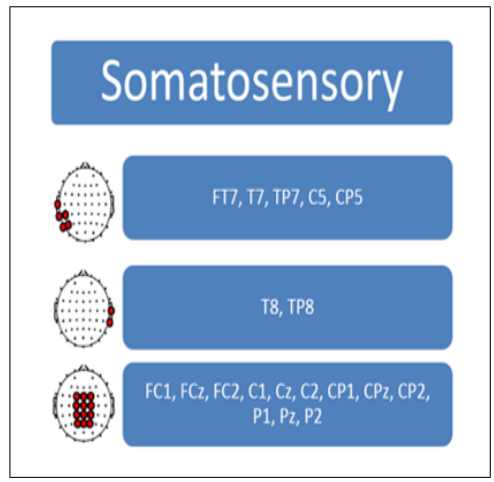

Figure 5.2: sROIs for somatosensory evoked potentials.

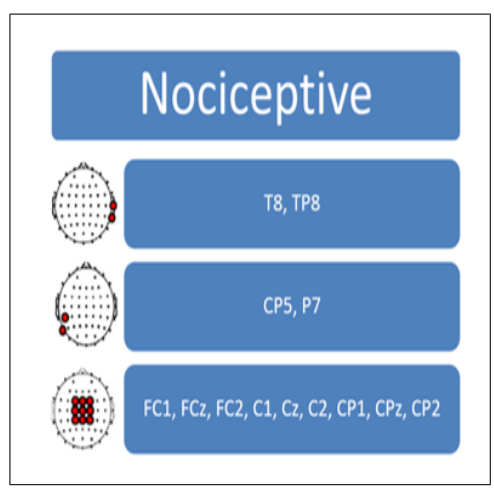

Figure 5.3: sROIs for nociceptive evoked potentials.

6

Methods

6.1 EEGLAB and independent component analysis (ICA)

EEGLAB is a toolbox and graphic user interface, running under the cross-platform MATLAB environment (The Mathworks, Inc.) for processing collection of single-trial and/or average EEG data of any number of channels. [22] Available functions include EEG data, channel and event information importing, data visualization, preprocessing, independent component analysis (ICA) and time/frequency decompositions including channel and component cross-coherence supported bootstrap statistical methods based on data resampling.

A primary tool of EEGLAB is to facilitate the process of applying and evaluating the results of independent component analysis of EEG data. ICA algorithms have proven capable of isolating both artifactual and neurally generated EEG sources whose EEG contributions, across the training data, are maximally independent of one another. ICA was first applied to EEG by Makeig et al. (1996) and is now widely used in the EEG research community, most often to detect and remove stereotyped eye, muscle, and line noise artifacts. ICA also has proved capable of separating biologically plausible brain sources whose activity patterns are distinctly linked to behavioral phenomena. In fact, many of the biologically plausible sources ICA identified in EEG data have scalp maps nearly fitting the projection of a single equivalent current dipole, and are therefore quite compatible with the projection to the scalp electrodes of synchronous local field activity within a connected patch of cortex.

EEGLAB contains an automated version, runica() of the infomax ICA algorithm with several enhancements both as a Matlab function and as a stand-alone binary C program that allows faster and less memory-intensive computation [22].

We can also study the relative strengths of the independent components projected back onto the scalp using topplot(). Make decisions on which independent components might be artifacts using generally accepted heuristics and finally remove selected artifacts using icaproj() [17].

Visualizing EEG artifacts

The function topplot() is used to study the relative strengths of the independent components projected back onto scalp. Assuming W is the weights matrix obtained after running the ICA algorithm, the columns of the inverse matrix, inv(W), give the relative projection strengths of the respective components at each of the scalp sensors. These plots helps in visualizing the components physiological origins [17]. Graphically the process looks as illustrated in the Fig. 6.1.

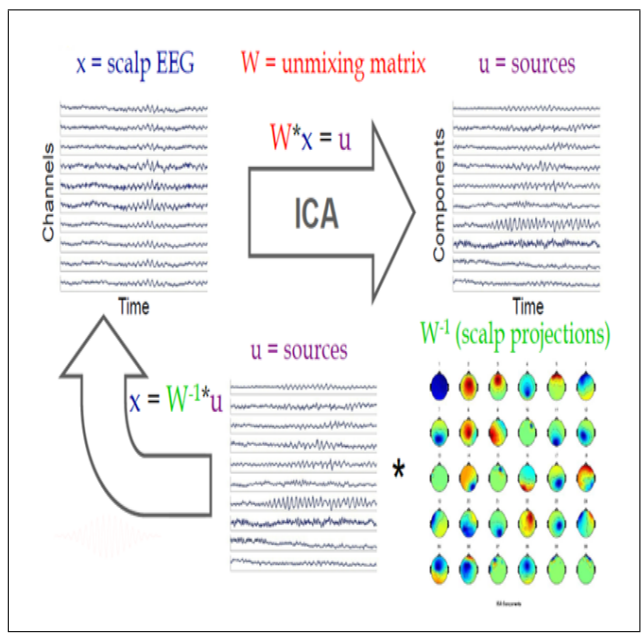

Figure 6.1: ICA [23].

Where every scalp map in the scalp projections is representing the coefficients a_{ij} from eq (4.3) for one independent component. In other words every scalp map is built from one column of matrix W^{-1} where the rows are related to the channels or EEG electrodes in this case, and the columns are related to sources or independent components, so for example the independent component 3 in Fig. 6.1 is represented by the the projection shown in Fig 6.2.

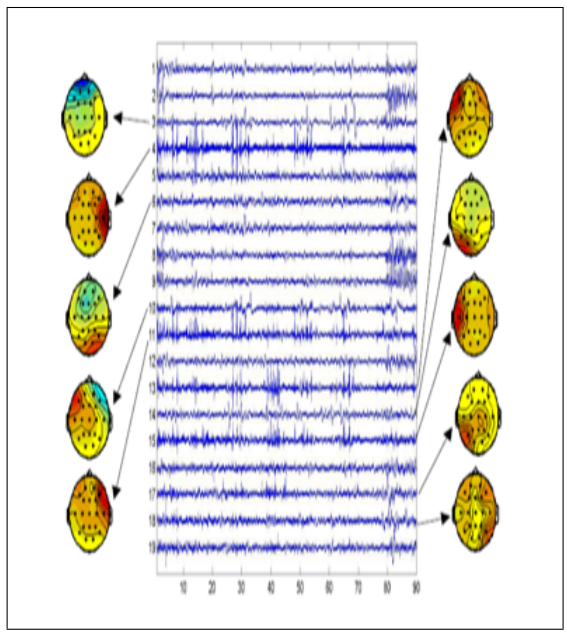

Figure 6.3: ICA components and projections of selected artifacts [17].

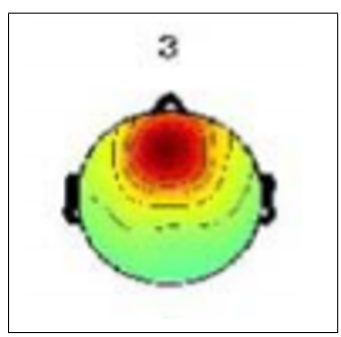

Figure 6.2: Scalp projection, component 3.

In this case we are plotting the third column from W^{-1}. Knowing certain properties of different artifacts help in deciding which components can be classified as probable artifacts [17]:

1. Eye movements and eye blinks mainly to frontal sites (near electrodes FP_1 and FP_2).

2. Temporal muscle activity should project to the temporal sites (near T_3 and T_4).

3. Occipital (rear head) movements project to the back (electrodes O_1 and O_4).

They should be projected as shown in Fig. 6.3.

Some of the scalp projections are clearly artifacts and not deep analysis

is required, however when using the EEGLAB plugin it is always possible to drill down the results in order to classify the independent components as an artifact or not. The scalp projections in EEGLAB/Matlab are plotted as shown in Fig. 6.4.

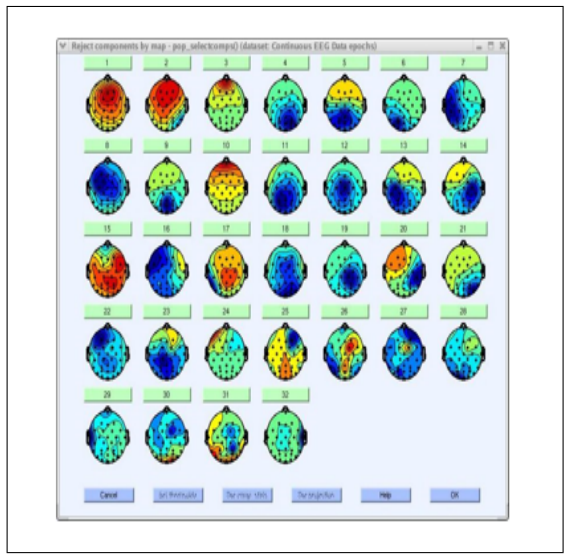

Figure 6.4: Scalp Projections EEGLAB [24].

And by clicking the rectangular button above each component one can access the properties of the components. For example the component 3 Fig. 6.4 can be identified as an eye artifact for three reasons [24]:

1. The smoothly decreasing EEG spectrum is typical of an eye artifact.

2. The scalp map shows a strong far-frontal projection typical of eye artifacts.

3. It is possible to see individual eye movements in the component when clicking in the top button to access the properties

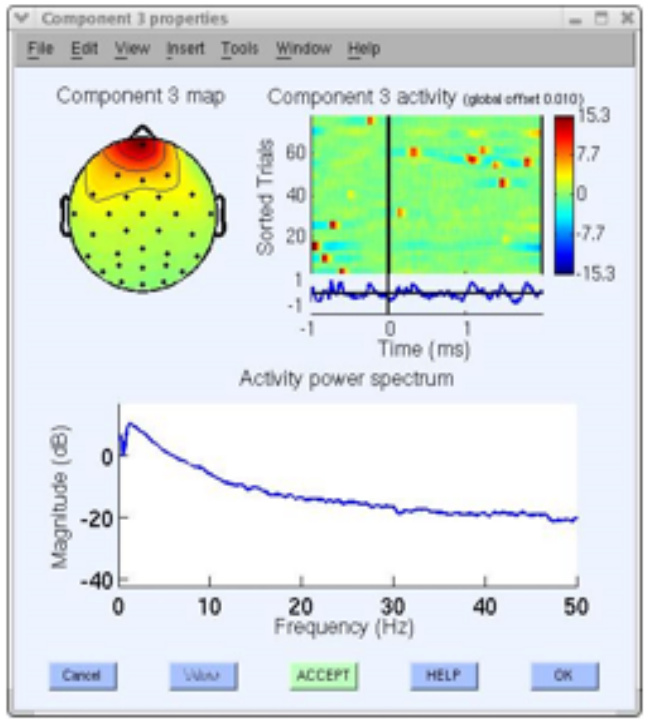

Figure 6.5: Component 3 properties [24].

Since this component accounts for eye activity, we may wish to subtract it from the data before further analysis and plotting. If so, click on the bottom green Accept button (above) to toggle it into a red Reject button. Now press OK to go back to the main component property window.

Another artifact example in our decomposition is component 32, which appears to be typical muscle artifact component. This components is spatially localized and show high power at high frequencies (20-50 Hz and above) as shown in Fig. 6.6.

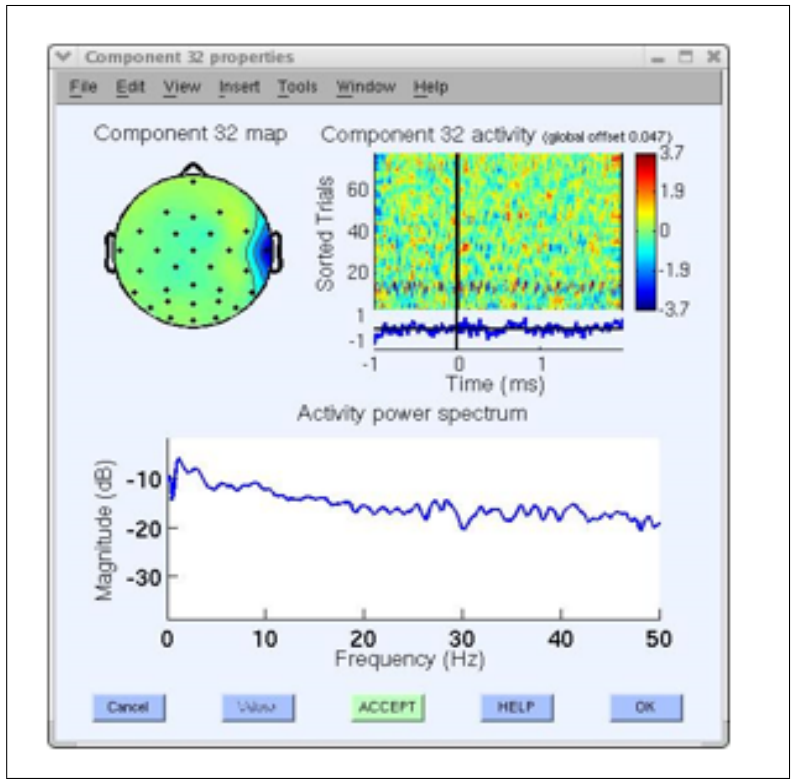

Figure 6.6: Component 32 properties [24].

Once the components to eliminate from the data are selected we can mix the new sources (without the components selected) and the weights back again, and as a result we obtain artifact rejected clean data as follows [17]:

clean data=$W^{-1}(:, a)\text{ica}(a, :)$

Where:

a=vector of independent components to keep

ica=independent components Obtain from $W \times X$

For example, let $H = \begin{bmatrix} 1 & 2 & 3 \\ 3 & 1 & 2 \\ 2 & 3 & 1 \end{bmatrix}$ be the blind mixing matrix on the blind sources $S = \begin{bmatrix} s_1 \\ s_3 \\ s_2 \end{bmatrix}$

producing the recorded EEG data $X = \begin{bmatrix} s_1 + 2s_2 + 3s_3 \\ 3s_1 + s_2 + 2s_3 \\ 2s_1 + 3s_2 + s_3 \end{bmatrix}$

Now, suppose we wanted to remove the independent component s_2 from the observed EEG data X. Then $a = [1\ 3]$

and clean data is,

$$\begin{aligned} \text{clean data}=W^{-1}(:, [13]) \times \text{ica}([13], :) \\ = H(:, [13]) \times X = \begin{bmatrix} s_1 s_3 \end{bmatrix} \\ = \begin{bmatrix} s_1 + 3s_3 \\ 3s_1 + 2s_3 \\ 2s_1 + s_3 \end{bmatrix} \end{aligned}$$

Graphically the process is explained by Fig. 6.7.

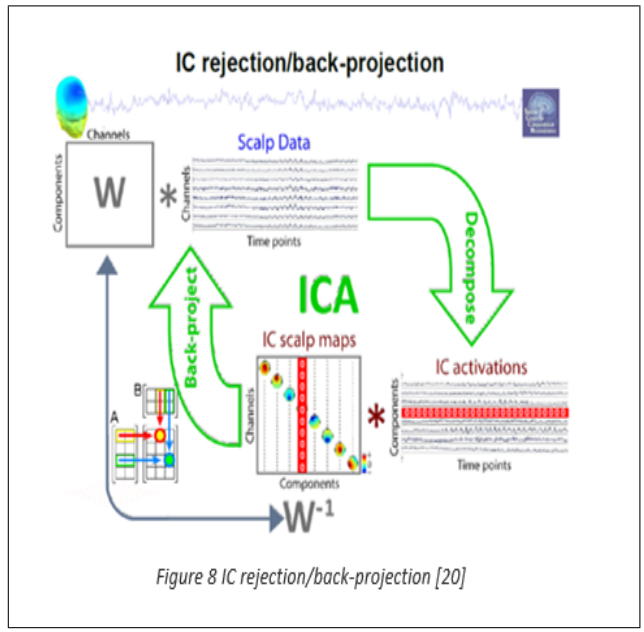

Figure 6.7: IC rejection/back-projection [23].

6.2 Artifact rejection

EEG data from 8 subjects, 8 recording blocks each (1 repeated block per condition: Nociceptive Active, Nociceptive Passive, Somatosensory Active, Somatosensory Passive), were processed using the EEGLAB toolbox. Firstly we applied a baseline correction to reduce the zero level fluctuations over the EEG signals across all channels, such fluctuations might be due to noise sources, sweating or muscles movement [25].

Then we used the Independent Component Analysis (ICA) to correct trials contaminated by eyes movement or muscles activity, and then we corrected baseline again to restore the zero level. Frontal scalp distribution activity affected most of the EEG recording blocks, temporal and occipital activations were found as well, indicating muscle artifacts and rear-head artifacts respectively [17].

For example in Fig. 6.8 we can see the projections for the sixth subject corresponding to the nociceptive active condition. Every scalp map in Fig. 6.8 corresponds to the projections of one of the independent components found after running the ICA algorithm, the value assigned to each one of the electrodes relies on the coefficients a_{ij} given by eq. 4.3.

If we drill down over the component 42 we can obtain the scalp projection (Fig. 6.9) and the power spectrum (Fig. 6.10) of such component.

There's clearly a pronounced activity over the occipital cortex suggesting a rear-head artifact. Furthermore occipital activity is characterized by an alpha band peak near 10 Hz [24] as we can see in the Fig. 6.10

Thus this component could be classified as a rare-head artifact. Frontal activity indicating eyes movement and/or eyes blinking were largely present in all subjects. In Fig. 6.11 we can see the scalp projection map corresponding to the first component of the the seventh subject for the nociceptive passive recording block for which could be classified as eyes movement artifact by its activity over the frontal region and when we plot the power spectrum Fig. 6.12 we can confirm so since it appears to be smoothly decreasing.

Besides, this activity should coincide with the activations of the electrooculography (EOG) signals which were simultaneously recorded from the four surface electrodes placed on the upper and lower eyelid, and next by the outer canthus of the left and right eye. Using EEGlab we can plot the data having eliminated this component as shown in Fig. 6.13.

Figure 6.13 shows a sample of the EEG data before (blue signals) and after (red signals) eliminating the component 1 from the data, this figure shows the results for 62 channels, the electrooculographic channels are numbered 22, 32, 39 and 62 for outer canthus left eye, lower eyelid, outer canthus right eye and upper eyelid respectively. By looking at the behavior of the electrooculographic channels we can see their activations characterized by an increase in the potential, in this case it is presented at about 300 ms after the stimulus.

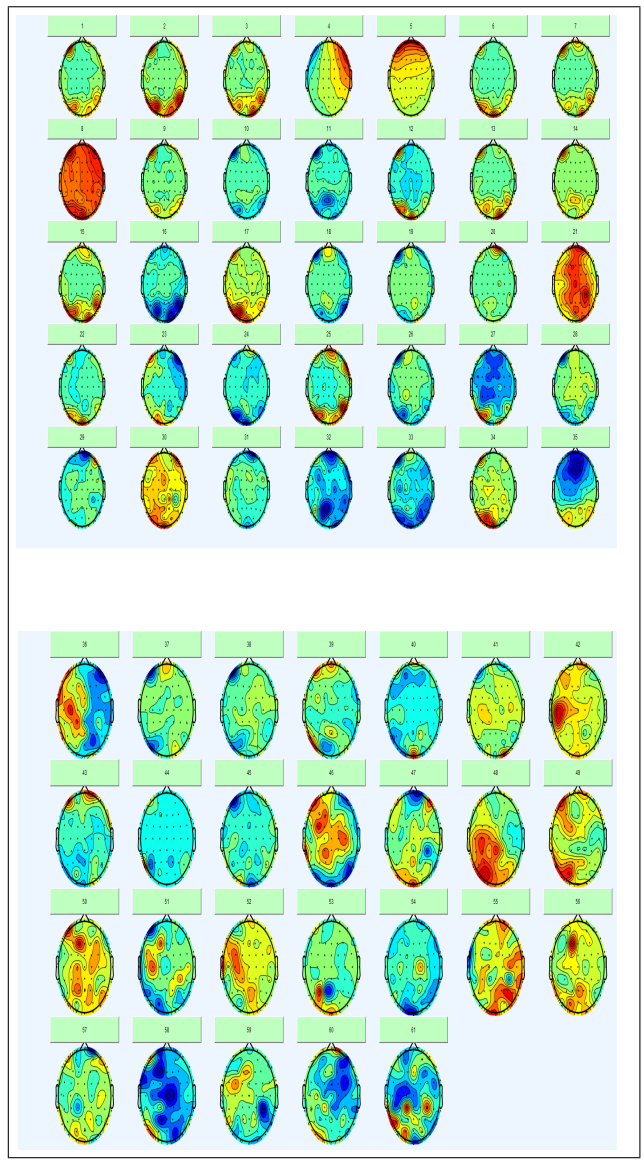

Figure 6.8: Projections, Subject 6, Nociceptive Active condition.

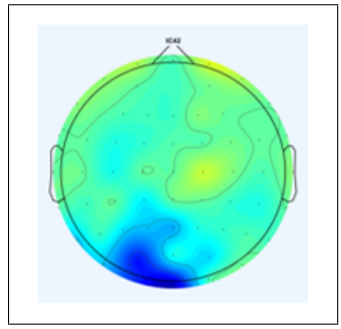

Figure 6.9: Scalp projection independent component 42.

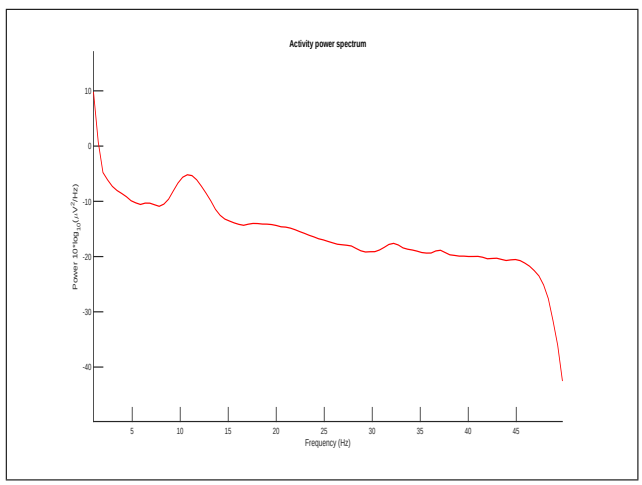

Figure 6.10: Power spectrum Independent component 42.

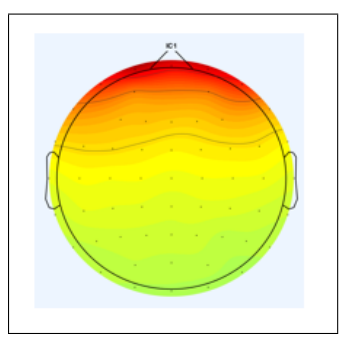

Figure 6.11: Scalp projection independent component 1.

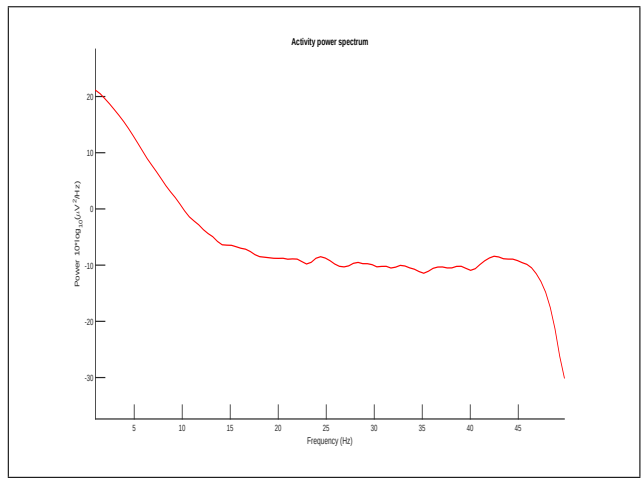

Figure 6.12: Power spectrum Independent component 1.

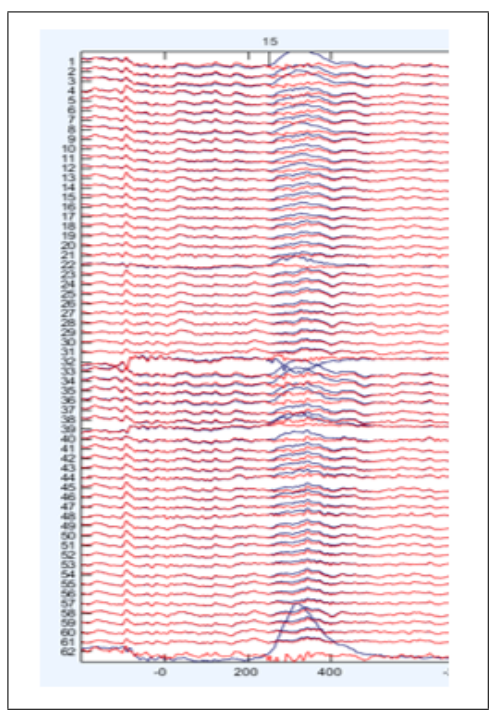

Figure 6.13: EEG data with and without component 1.

At the same time we can inspect how this component is eliminated from all of the channels by comparing the blue and the red signals, being the red signal the one representing the corrected data.

Artifacts related to muscle movement were also found in the data. In Fig. 6.14 we present the last 27 components for the sixth subject corresponding to the nociceptive passive condition, for which we plot the properties of the component 57 (Fig. 6.15 and Fig. 6.16). If we take a look at its scalp projection (Fig. 6.15) we can see activity over the T4 electrode and temporal region, then it might be possible to classify this component as a muscle movement artifact. We can confirm so by plotting its power spectrum (Fig. 6.16) and checking once again if it matches with an artifact.

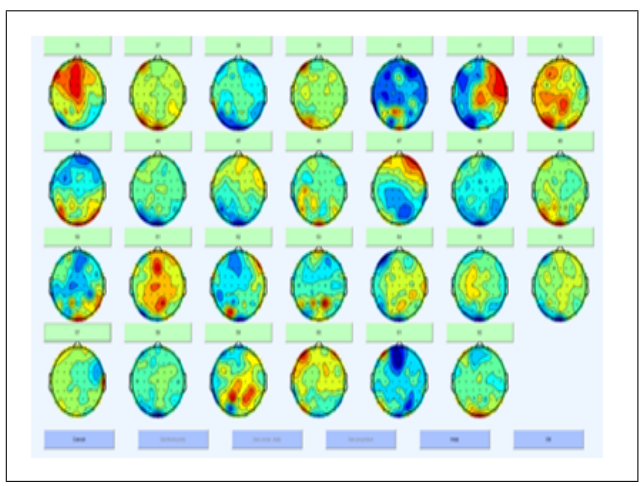

Figure 6.14: Projections, Subject 6, Nociceptive Passive condition.

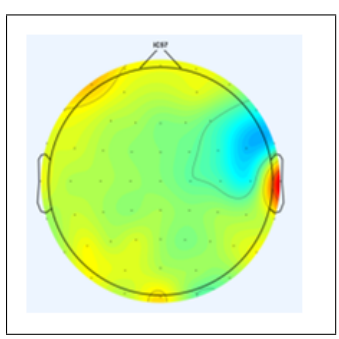

Figure 6.15: Scalp projection independent component 57.

The high power at high frequencies over 20Hz allows us to classify this component as a muscle movement artifact. Thus, this type of components

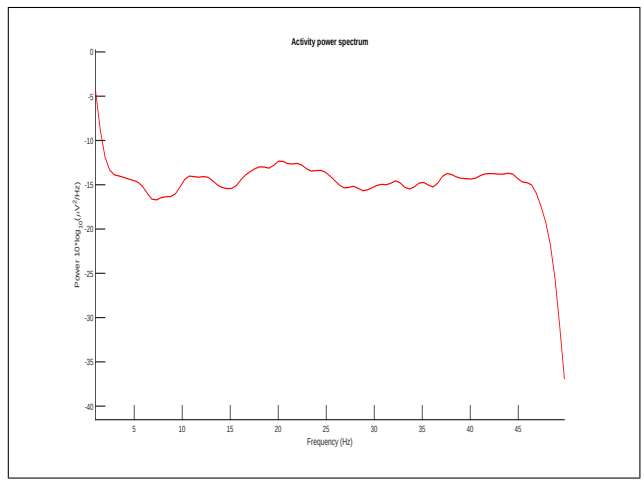

Figure 6.16: Power Spectrum component 57.

were removed from the original EEG data. In total 3968 components were analyzed across all subjects.

6.3 EP's Extraction

After that, we were able to extract the evoked potentials for each recording block, bearing in mind that according to the experiment setup and the roving paradigm in which it was based on, there were two different types of evoked potentials: those evoked by a standard stimulus and those evoked by a deviant stimulus.

For the evoked potentials we took time windows of 700ms, 200ms for pre-stimulus and 500ms for post-stimulus over each channel [21]. For each recording block and each channel there were 50 stimuli of every type (50 deviant stimuli and 50 standard stimuli) which were averaged. In order to estimate whether it was reasonable or not to average across subjects we first obtained the standard deviation for each subject, condition and type of stimulus between the evoked potentials for the channels belonging to the same region of interest. In Fig. 6.17 we can see the deviant evoked potentials read from the channels FT7,T7,TP7,C5 and CP5 (contralateral temporal region) of one of the subjects, during the somatosensory passive recording block. There is also shown the mean value across the channels and the standard deviation:

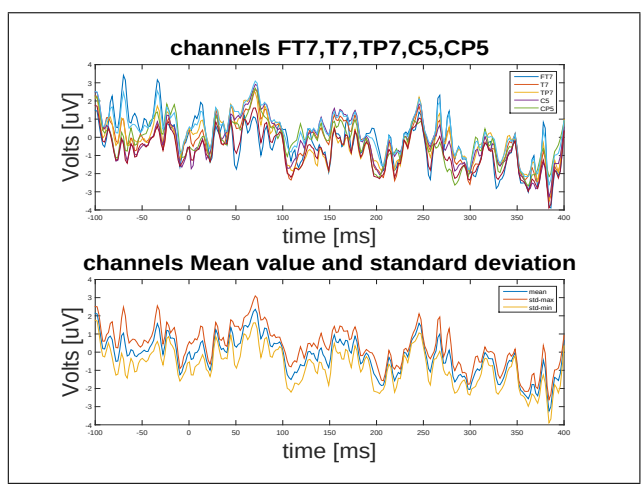

Figure 6.17: ERP channels FT7,T7,TP7,C5 and CP5

We then computed the standard deviation point by point across the time axis and averaged the resulting vector. Finally we average the results across all subjects. In fig. 6.17 we can see the evoked potentials look so similar as expected since both channels belong to the same region of interest. The results are shown later on chapter 7

After that we were able to average such evoked potentials resulting in one single evoked potential for each subject, condition, type of stimulus, and region of interest

Consequently we grouped the evoked potentials across all subjects, once

again the evoked potentials were grouped according to the condition, type of stimulus and region of interest they belonged to so we could average the evoked potentials and obtain the resulting evoked potential which will describe the response for one condition, one type of stimulus and one region of interest. Evoked potentials results are shown in chapter 7.

6.4 Wavelet transform

Since our purpose is to make an analysis on the time-frequency domain we computed a wavelet transform using the Gabor transform for each evoked potential in the groups (each group containing the evoked potentials for each subject separately) and calculated the standard deviation between the results.

Then we averaged the Gabor windows for each group. The result of all this operation is a Gabor window by condition, type of stimulus and region of interest.

Once we had that, we could start making comparisons between the Gabor windows obtained. We were interested in comparing the difference between a standard stimulus and deviant stimulus within each condition as well as the difference between the conditions for both the deviant and standard stimulus.

The comparisons were made by pairs. We computed the difference between the different Gabor windows, if the difference was greater than the standard deviation found for the Gabor windows we were comparing, then the results were considered as significant.

7

Results

Let us start saying that the results for the standard deviation allowed us to keep the regions of interest found in [21] showing similar responses for the channels belonging to the same region of interest. The results are shown in the tables 7.1, 7.2, 7.3 and 7.4 .

Table 7.1: Standard deviation results Nociceptive Active Condition

Type of stimulus	Central region	Contralateral temporal region	Ipsilateral
Deviant	1.05	0.84	1.01.
Standard	1.18	0.88	1.13

(Values in μV)

Table 7.2: Standard deviation results Nociceptive Passive Condition

Type of stimulus	Central region	Contralateral temporal region	Ipsilateral
Deviant	0.82	0.82	1.00
Standard	0.87	0.67	0.88

(Values in μV)

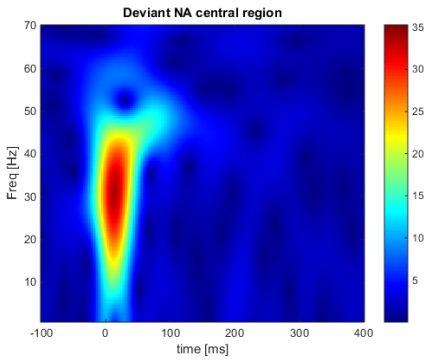

(a) Central region, deviant stimulus

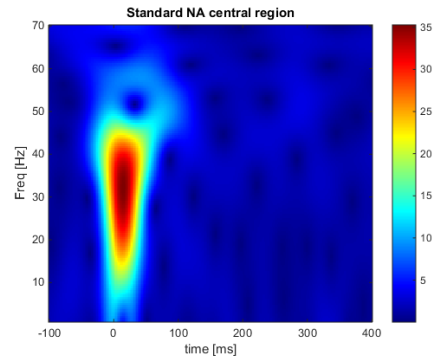

(b) Central region, standard stimulus

Figure 7.1: Gabor window, Deviant and Standard stimulus

Table 7.3: Standard deviation results Somatosensory Active Condition

Type of stimulus	Central region	Contralateral temporal region	Ipsilateral
Deviant	1.56	1.45	0.80
Standard	1.10	1.08	1.87

(Values in μV)

Table 7.4: Standard deviation results Somatosensory Passive Condition

Type of stimulus	Central region	Contralateral temporal region	Ipsilateral
Deviant	0.94	0.97	0.68
Standard	0.92	0.90	0.64

(Values in μV)

7.1 Nociceptive active condition

In Fig. 7.1 we can see the Gabor window for both the deviant stimulus and standard stimulus for the central region. These two Gabor windows are plotted using the same scale in order for them to be compared. If we take look at these two windows we will probably not find any significant difference.

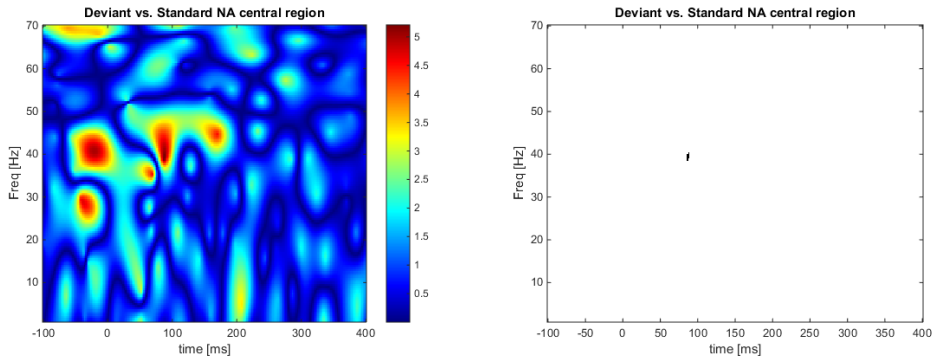

(a) Central region, deviant - standard stimulus

(b) Central region, deviant - standard stimulus, significant values

Figure 7.2: Deviant vs. Standard stimulus

However, for us to be able to find the differences between these two Gabor windows we computed the mathematical difference pixel by pixel and obtained the result showed in Fig. 7.2a where we can clearly appreciate the main differences for each value in the matrices.

In this case we found the biggest difference around 40 Hz for both the pre-stimulus at a latency of 20ms before stimulus and in the post-stimulus at a latency of 88ms. It was expected not to have the same Gabor window for the standard and deviant stimulus. In spite of the fact that the results are different, the differences might not be significant enough compared to the standard deviation found for each Gabor Window.

For that reason in Fig. 7.2b we plotted only the pixels of the Gabor window in Fig. 7.2a whose values were larger than the largest value of the standard deviation of the Gabor windows in Fig. 7.1a. In this case the standard deviation for the Gabor window in Fig. 7.1a was 5.09 and 5.02 for Fig. 7.1b, so in Fig. 7.2b we only plotted the pixels with values larger than 5.09.

As shown in Fig. 7.2b no significant results were found. Aftermath the evoked potentials must be very similar between each other and indeed they are as we can see in Fig. 7.3

The same procedures were applied for the other regions of interest and conditions. In Fig. 7.4 we can see the Gabor windows for the deviant and standard stimulus for the contralateral temporal region. And in Fig. 7.5 we can see the difference between these two Gabor windows. This time the results show significant values during the pre-stimulus for frequencies near the 40Hz (Fig. 7.5b), and once again we can appreciate the result in the time-domain shown in Fig. 7.6, however in this case the time-domain graphic does not offer as much information.

For the case of the contralateral temporal region and the ipsilateral region

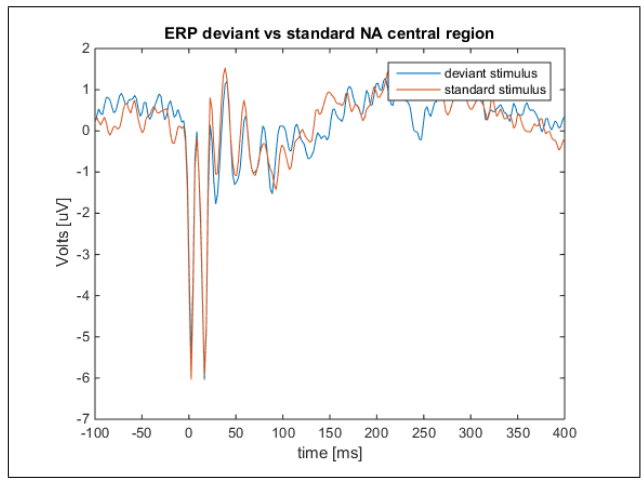

Figure 7.3: Central region EP's, deviant and standard stimulus

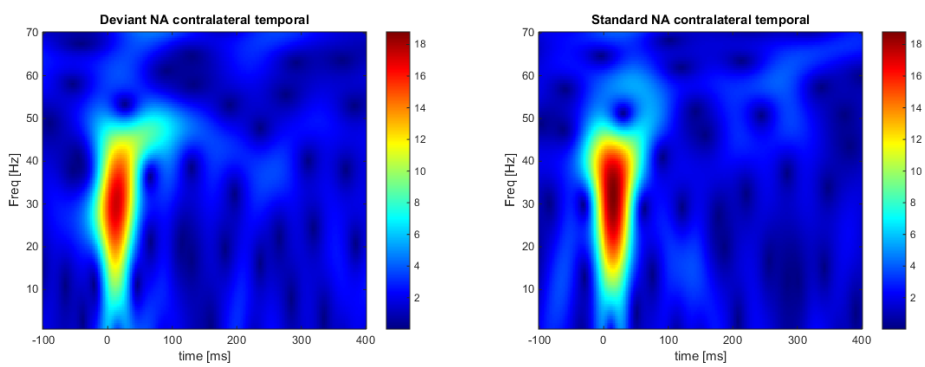

(a) contralateral-temporal region, deviant stimulus

(b) contralateral-temporal region, standard stimulus

Figure 7.4: Gabor window, Deviant and Standard stimulus

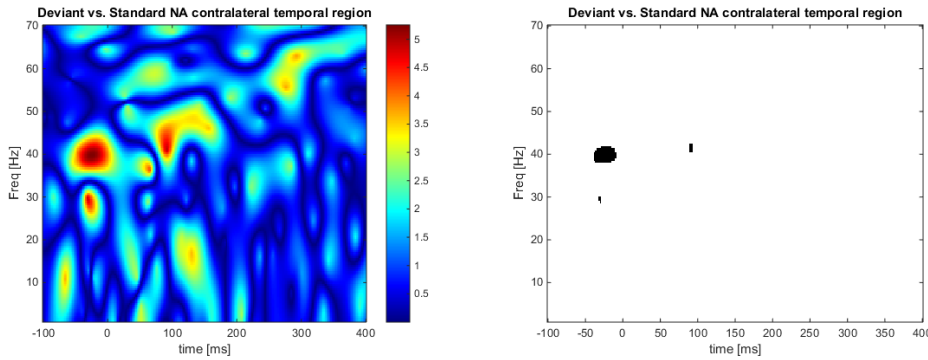

(a) contralateral-temporal region, deviant - standard stimulus

(b) contralateral-temporal region, deviant - standard stimulus, significant values

Figure 7.5: Deviant vs. Standard stimulus

we obtained similar responses, but still not very significant. For the case of the ipsilateral region the main difference was found once again around the 40 Hz 24 seconds before the stimulus.

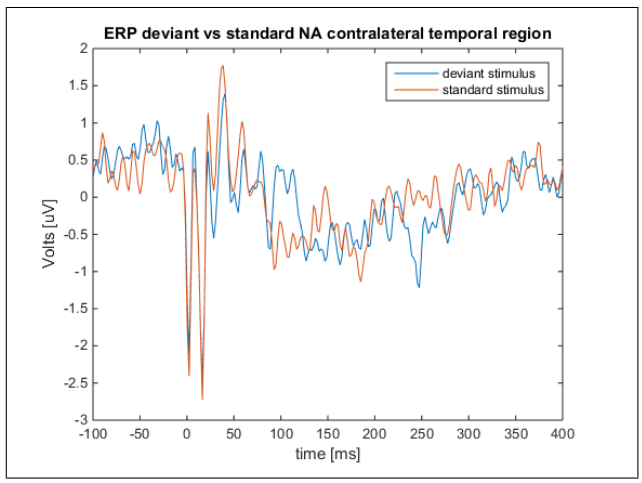

Figure 7.6: contralateral-temporal region EP's, deviant and standard stimulus

7.2 Nociceptive passive condition

For the nociceptive passive condition the results over the central region were not much different from the result obtained in the nociceptive active condition. The Gabor windows for the deviant and standard stimuli (Fig. 7.7) were so similar that there were not significant results when we computed the differences between them (Fig. 7.8) and as expected neither the evoked potentials showed big differences (Fig. 7.9).

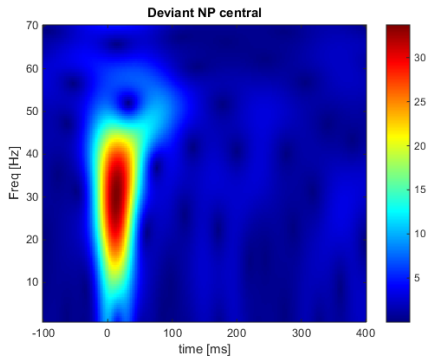

(a) Central region, deviant stimulus

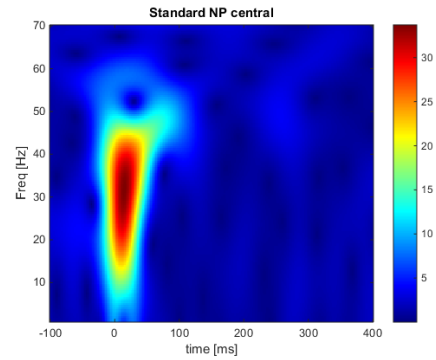

(b) Central region, standard stimulus

Figure 7.7: Gabor window, Deviant and Standard stimulus

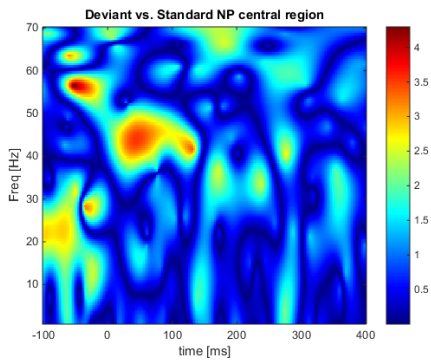

(a) Central region, deviant - standard stimulus

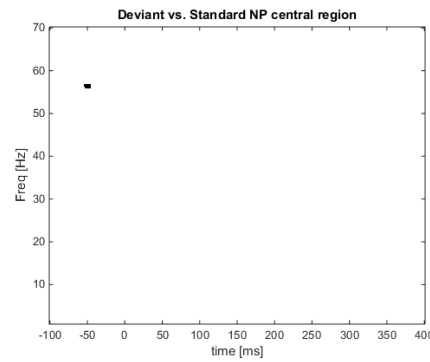

(b) Central region, deviant - standard stimulus, significant values

Figure 7.8: Deviant vs. Standard stimulus

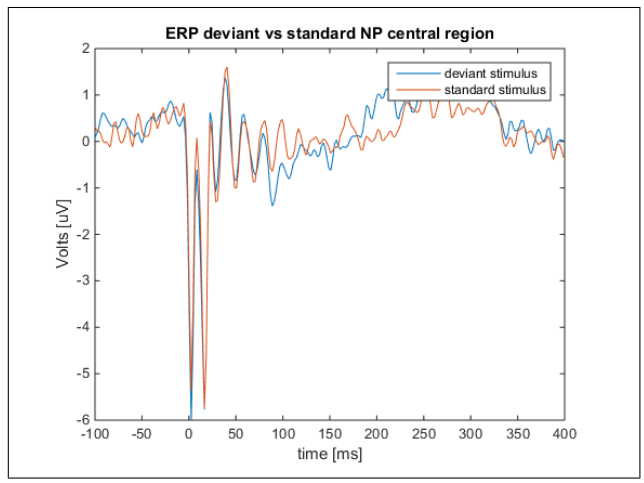

Figure 7.9: Central region EP's, deviant and standard stimulus

The results over the temporal regions (Fig. 7.10) were also similar between the deviant and standard stimuli and there were not significant values obtained in the Gabor window representing the mathematical difference between them.

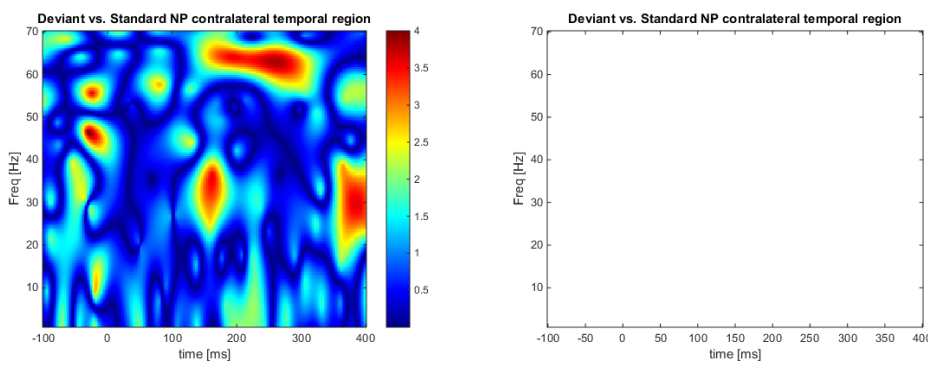

(a) contralateral-temporal region, deviant - standard stimulus

(b) contralateral-temporal region, deviant - standard stimulus, significant values

Figure 7.10: Deviant vs. Standard stimulus

7.3 Somatosensory Active condition

Similar situation is presented for the somatosensory condition but slightly different. First of all this time we did obtained significant difference over the central region for the active condition (Fig. 7.12) when we computed the differences between the Gabor windows in Fig. 7.11. Secondly, we also

obtained significant values over the temporal regions when comparing the deviant and standard stimuli for the active condition but we did not find significant values for the passive condition.

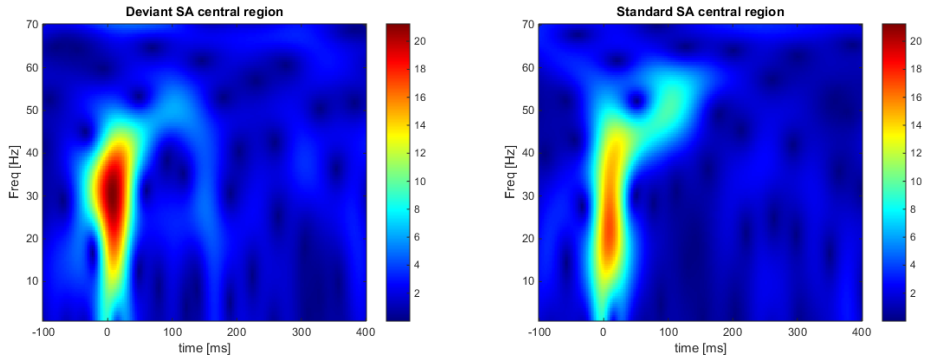

(a) Central region, deviant stimulus (b) Central region, standard stimulus

Figure 7.11: Gabor window, Deviant and Standard stimulus

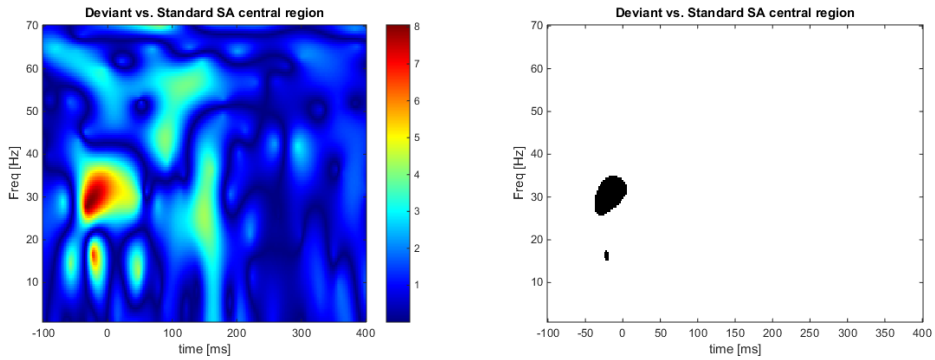

(a) Central region, deviant - standard stimulus

(b) Central region, deviant - standard stimulus, significant values

Figure 7.12: Deviant vs. Standard stimulus

This time the the main differences between the standard and deviant stimuli were found around the 30Hz with a latency of 22ms before the stimulus. Pretty much the same results were obtained for the temporal regions, in Fig. 7.13 and Fig. 7.14 we can appreciate the significant values around 30Hz during the pre-stimulus interval.

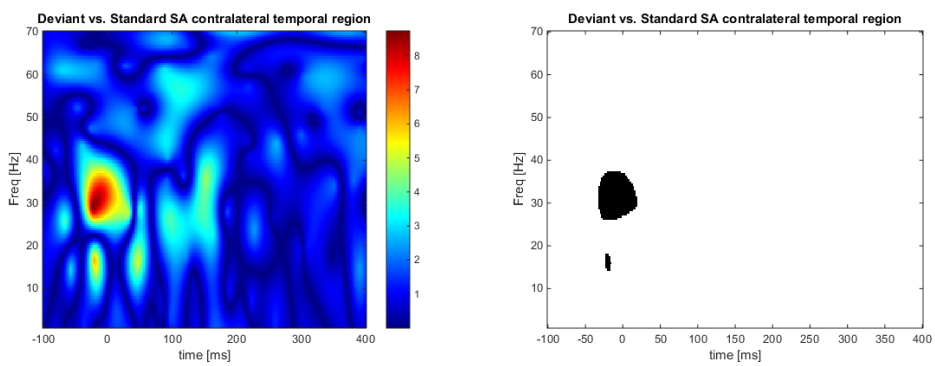

(a) contralateral-temporal region, deviant - standard stimulus

(b) contralateral-temporal region, deviant - standard stimulus, significant values

Figure 7.13: Deviant vs. Standard stimulus

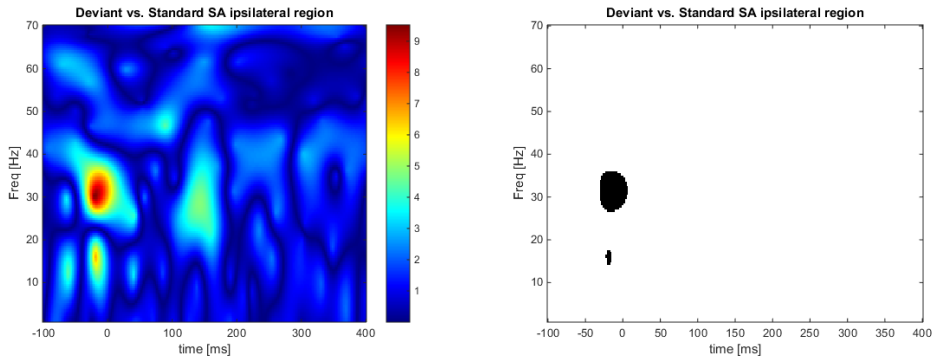

(a) ipsilateral region, deviant - standard stimulus

(b) ipsilateral region, deviant - standard stimulus, significant values

Figure 7.14: Deviant vs. Standard stimulus

7.4 Somatosensory Passive condition

As it was mentioned before, we did obtain significant values for the somatosensory active condition but it was not likewise for the somatosensory passive and as we can see in Fig. 7.15 where despite of the difference found between the deviant and standard Gabor windows, none of those differences were really significant.

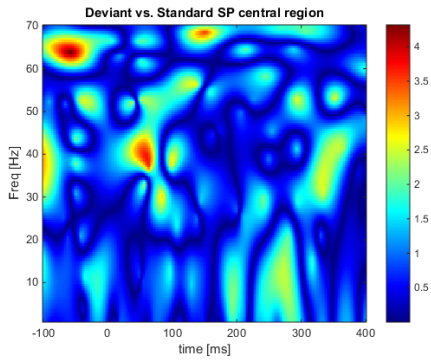

(a) Difference Gabor window

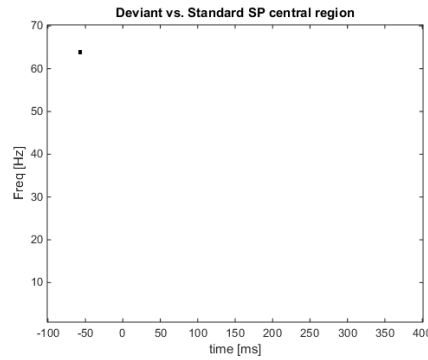

(b) Significant values Gabor window

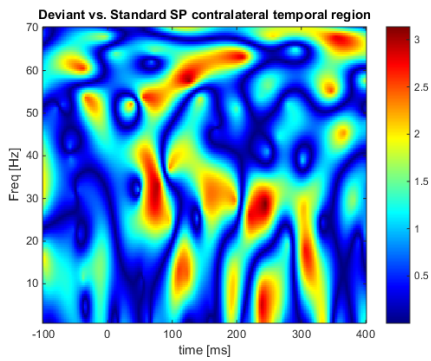

(c) Difference Gabor window

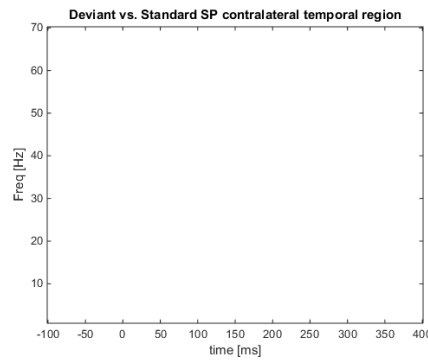

(d) Significant values Gabor window

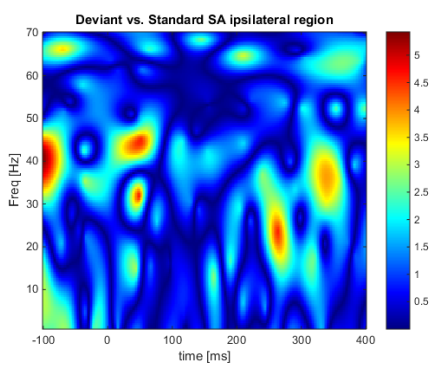

(e) Difference Gabor window

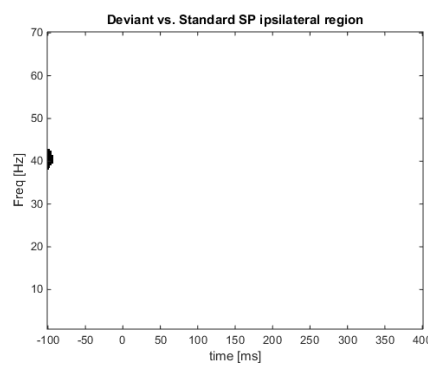

(f) Significant values Gabor window

Figure 7.15: Deviant vs. Standard stimulus, (7.15a) difference Gabor window over central region,(7.15b) significant values Gabor window over central region, (7.15c) difference Gabor window over contralateral-temporal region, (7.15d) significant values Gabor window over contralateral-temporal region, (7.15e) difference Gabor window over ipsilateral region, (7.15f) significant values Gabor window over ipsilateral region

7.5 Nociceptive vs. Somatosensory responses

To support the idea that there is, in fact, a difference between the responses evoked by nociceptive and somatosensory stimulation we also computed the differences for the Gabor windows of the nociceptive and somatosensory conditions as follows: nociceptive active condition vs somatosensory active condition, and nociceptive passive condition vs somatosensory passive condition. This time we assume that the factor of attention will not affect the result of the comparisons since it is the same for the recording blocks we are comparing, and thus we will only focus on the nociceptive vs somatosensory matter.

Nociceptive Active vs Somatosensory Active

Let us start with the nociceptive active condition vs somatosensory active condition comparison, which was also performed over the three regions of interest.

In the central region the Gabor windows were widely different for both the standard and deviant stimulus (Fig. 7.16 and Fig. 7.17). The difference were found from 10Hz to 60Hz and latency from 30ms before the stimulus to 96ms after the stimulus for the deviant stimulus, and from 8Hz to 62 Hz and latency from 46ms before the stimulus to 70ms after the stimulus for the standard stimulus. These results were also consistent with the evoked potential which show different responses (Fig. 7.18).Same result was persistent over the three regions of interest as shown from Fig. 7.19 to Fig. 7.24.

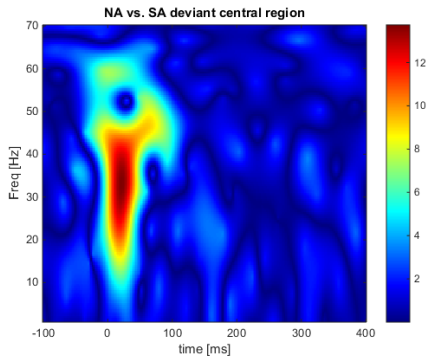

(a) Central region, deviant stimulus, Nociceptive active vs. Somatosensory active

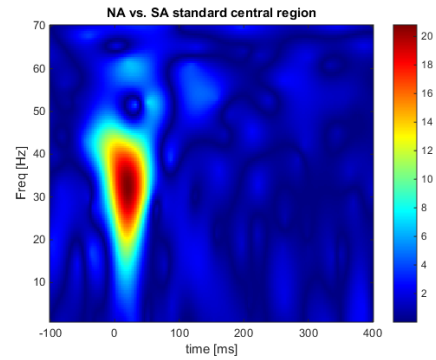

(b) Central region, standard stimulus, Nociceptive active vs. Somatosensory active

Figure 7.16: Gabor windows, Nociceptive active vs. Somatosensory active

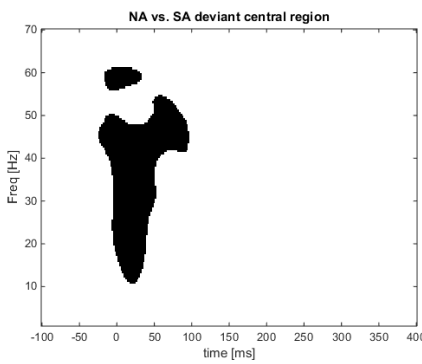

(a) Central region, deviant stimulus, Nociceptive active vs. Somatosensory active

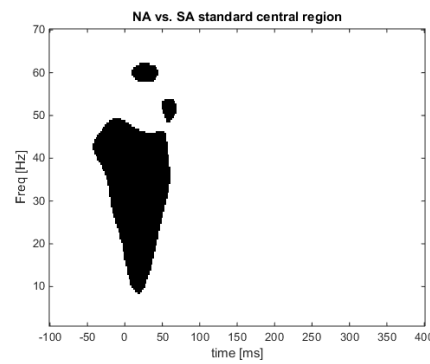

(b) Central region, standard stimulus, Nociceptive active vs. Somatosensory active

Figure 7.17: Significant Gabor windows, Nociceptive active vs. Somatosensory active

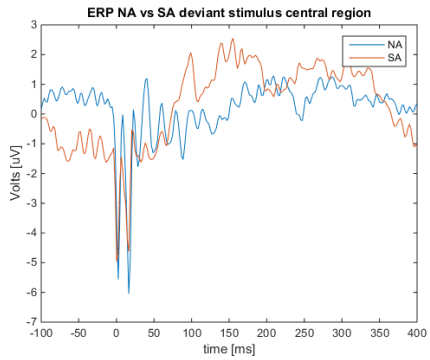

(a) Central region, deviant stimulus, Nociceptive active vs. Somatosensory active

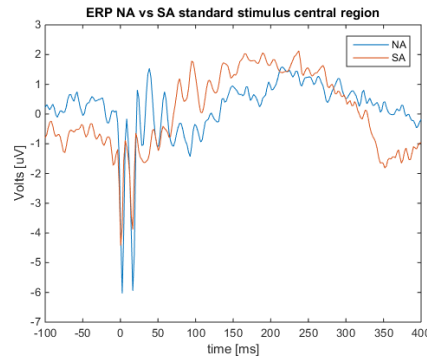

(b) Central region, standard stimulus, Nociceptive active vs. Somatosensory active

Figure 7.18: EP's, Nociceptive active vs. Somatosensory active

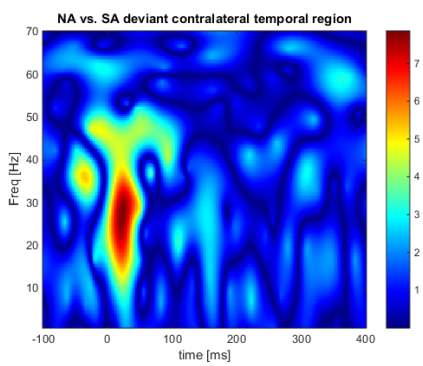

(a) contralateral-temporal region, deviant stimulus, Nociceptive active vs. Somatosensory active

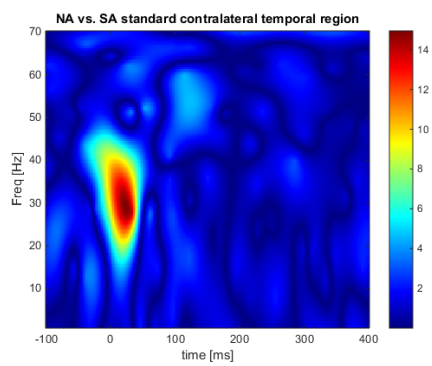

(b) contralateral-temporal region, standard stimulus, Nociceptive active vs. Somatosensory active

Figure 7.19: Gabor windows, Nociceptive active vs. Somatosensory active

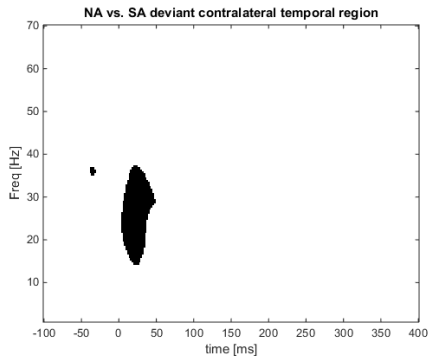

(a) contralateral-temporal region, deviant stimulus, Nociceptive active vs. Somatosensory active

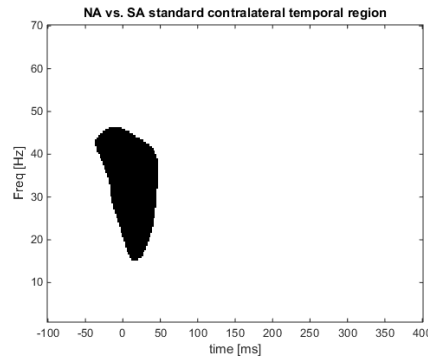

(b) contralateral-temporal region, standard stimulus, Nociceptive active vs. Somatosensory active

Figure 7.20: Significant Gabor windows, Nociceptive active vs. Somatosensory active

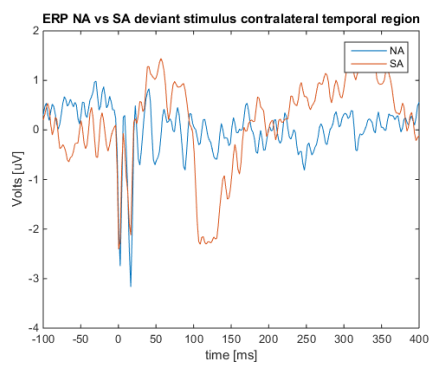

(a) contralateral-tempora region, deviant stimulus, Nociceptive active vs. Somatosensory active

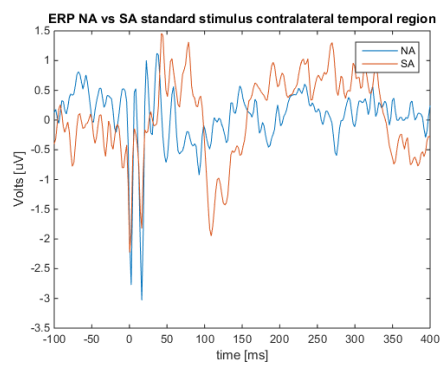

(b) contralateral-temporal region, standard stimulus, Nociceptive active vs. Somatosensory active

Figure 7.21: EP's, Nociceptive active vs. Somatosensory active

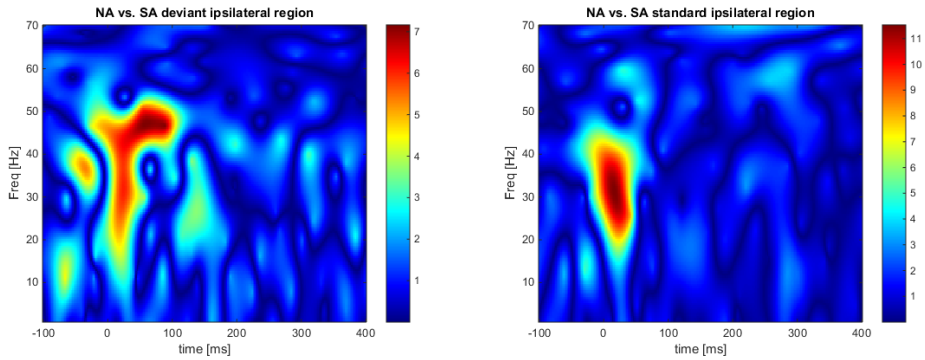

(a) ipsilateral region, deviant stimulus, Nociceptive active vs. Somatosensory active

(b) ipsilateral region, standard stimulus, Nociceptive active vs. Somatosensory active

Figure 7.22: Gabor windows, Nociceptive active vs. Somatosensory active

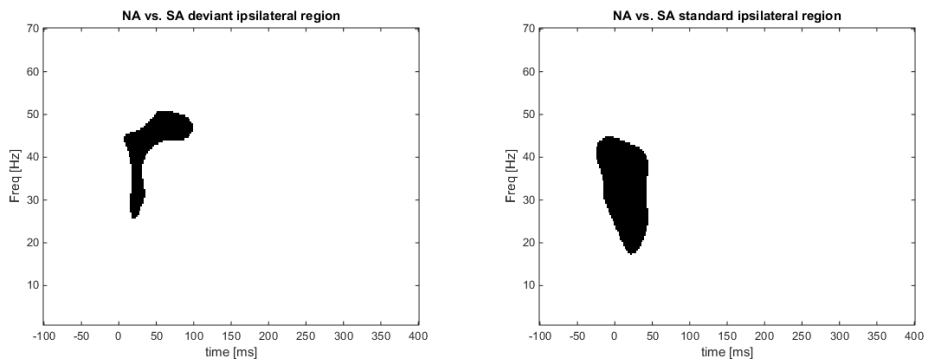

(a) ipsilateral region, deviant stimulus, Nociceptive active vs. Somatosensory active

(b) ipsilateral region, standard stimulus, Nociceptive active vs. Somatosensory active

Figure 7.23: Significant Gabor windows, Nociceptive active vs. Somatosensory active

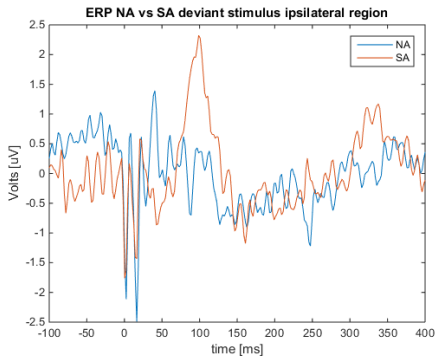

(a) ipsilateral region, deviant stimulus, Nociceptive active vs. Somatosensory active

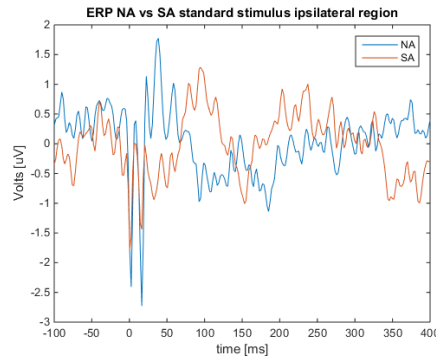

(b) ipsilateral region, standard stimulus, Nociceptive active vs. Somatosensory active

Figure 7.24: EP's, Nociceptive active vs. Somatosensory active

Nociceptive Passive vs. the Somatosensory Passive

In the central region the frequencies representing significant difference are in the range from 5Hz to 62Hz for the deviant stimulus and from 3Hz to 63Hz for the standard stimulus (Fig. 7.26). On the other hand for the temporal regions the range of frequencies representing significant difference in the Gabor windows was not as large but yet represent a wide frequency range, these results regarding the temporal regions are also shown in Figs. 7.28 to 7.33.

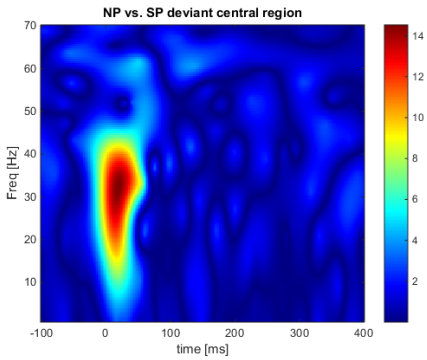

(a) Central region, deviant stimulus, Nociceptive passive vs. Somatosensory passive

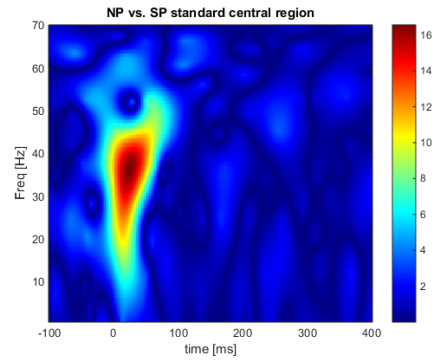

(b) Central region, standard stimulus, Nociceptive passive vs. Somatosensory passive

Figure 7.25: Gabor windows, Nociceptive passive vs. Somatosensory passive

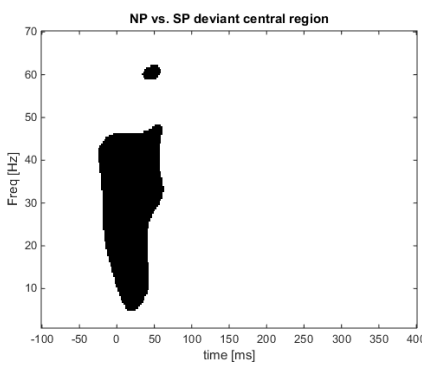

(a) Central region, deviant stimulus, Nociceptive passive vs. Somatosensory passive

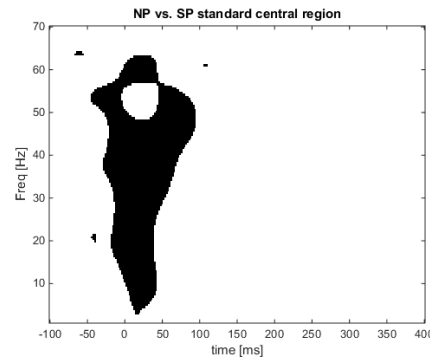

(b) Central region, standard stimulus, Nociceptive passive vs. Somatosensory passive

Figure 7.26: Significant Gabor windows, Nociceptive passive vs. Somatosensory passive

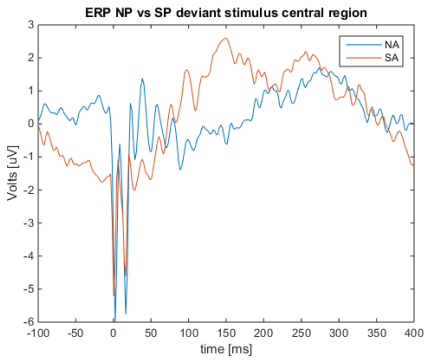

(a) Central region, deviant stimulus, Nociceptive passive vs. Somatosensory passive

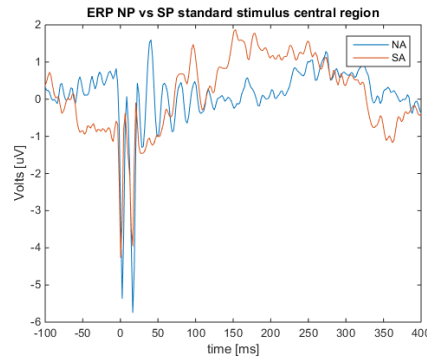

(b) Central region, standard stimulus, Nociceptive passive vs. Somatosensory passive

Figure 7.27: EP's, Nociceptive passive vs. Somatosensory passive

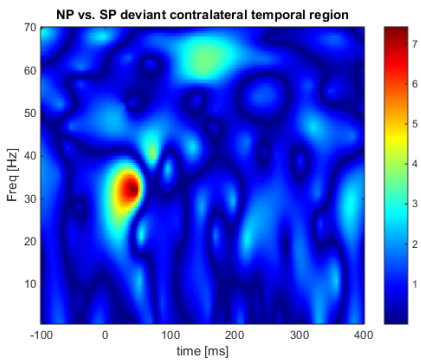

(a) contralateral-temporal region, deviant stimulus, Nociceptive passive vs. Somatosensory passive

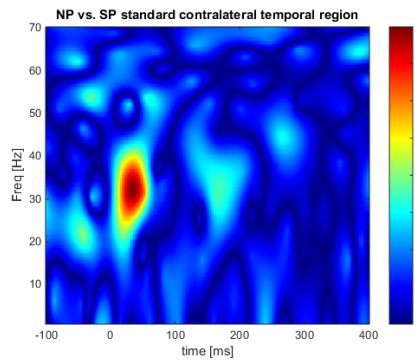

(b) contralateral-temporal region, standard stimulus, Nociceptive passive vs. Somatosensory passive

Figure 7.28: Gabor windows, Nociceptive passive vs. Somatosensory passive

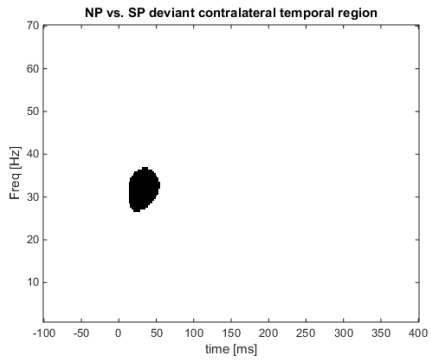

(a) contralateral-temporal region, deviant stimulus, Nociceptive passive vs. Somatosensory passive

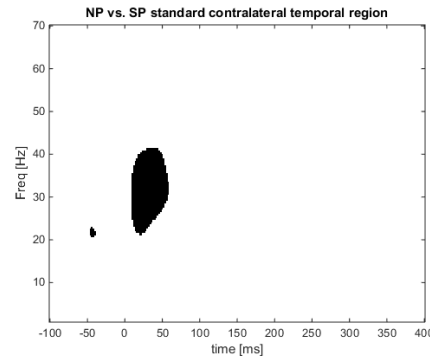

(b) contralateral-temporal region, standard stimulus, Nociceptive passive vs. Somatosensory passive

Figure 7.29: Significant Gabor windows, Nociceptive passive vs. Somatosensory passive

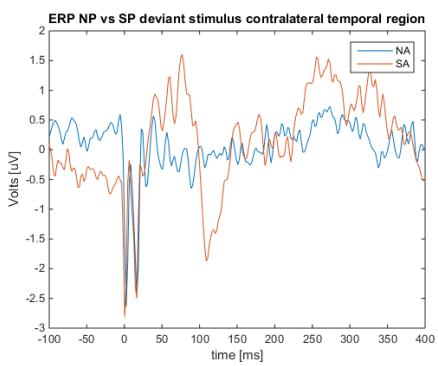

(a) contralateral-temporal region, deviant stimulus, Nociceptive passive vs. Somatosensory passive

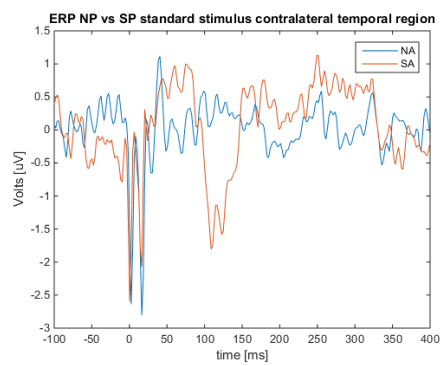

(b) contralateral-temporal region, standard stimulus, Nociceptive passive vs. Somatosensory passive

Figure 7.30: EP's, Nociceptive passive vs. Somatosensory passive

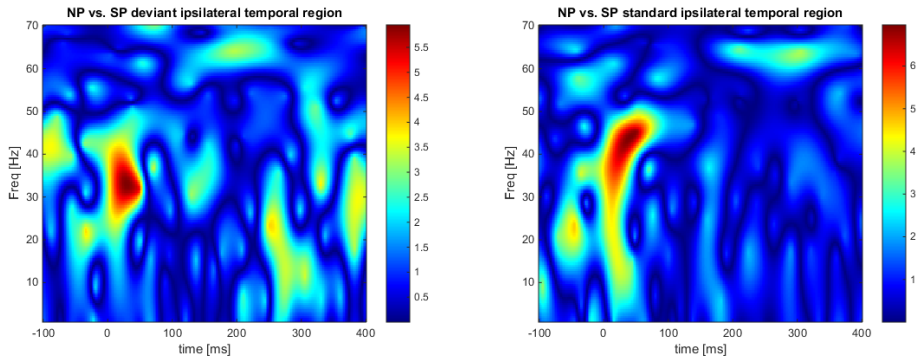

(a) ipsilateral region, deviant stimulus, Nociceptive passive vs. Somatosensory passive

(b) ipsilateral region, standard stimulus, Nociceptive passive vs. Somatosensory passive

Figure 7.31: Gabor windows, Nociceptive passive vs. Somatosensory passive

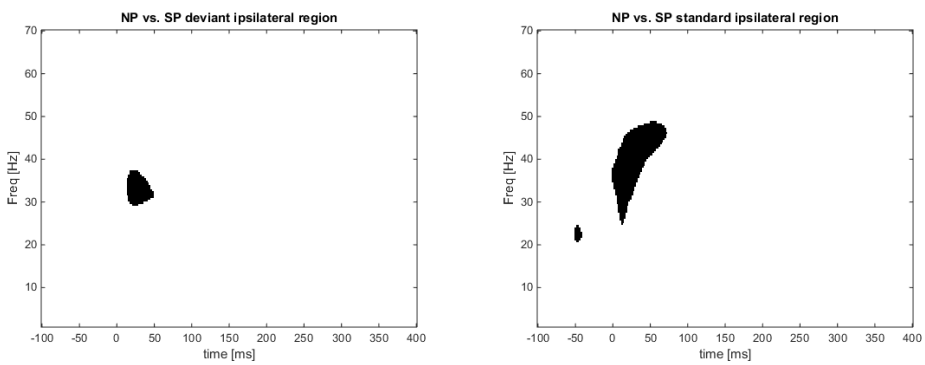

(a) ipsilateral region, deviant stimulus, Nociceptive passive vs. Somatosensory passive

(b) ipsilateral region, standard stimulus, Nociceptive passive vs. Somatosensory passive

Figure 7.32: Significant Gabor windows, Nociceptive passive vs. Somatosensory passive

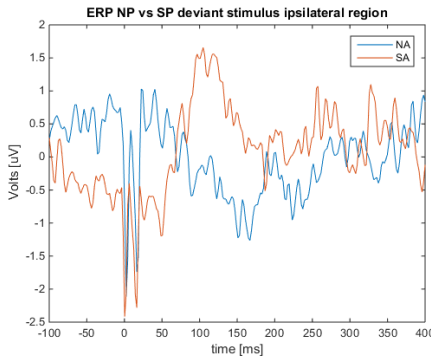

(a) ipsilateral region, deviant stimulus, Nociceptive passive vs. Somatosensory passive

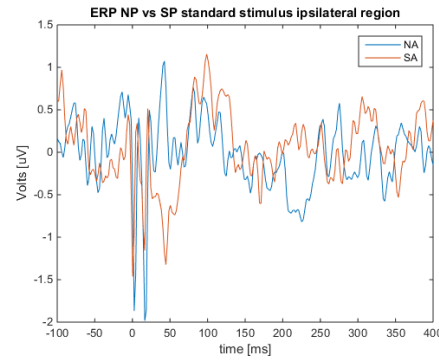

(b) ipsilateral region, standard stimulus, Nociceptive passive vs. Somatosensory passive

Figure 7.33: EP's, Nociceptive passive vs. Somatosensory passive

8

Discussion

During the nociceptive active condition there was no difference between the standard and deviant stimulus results found in the central region, there was no antiphase nor differences in the amplitude observed in the evoked potentials, which suggests that when it comes to nociceptive stimulation there are not many differences in how the deviant and standard stimuli are reflected over the cortex, in this case over the central region. For the temporal regions the main differences were found around 40Hz, 24 seconds before the stimulus.For both regions the result was consistent. In this case it is interesting to see a response over the pre-stimulus bearing in mind that the participants were on the active condition which means they were actually focusing on the stimuli before those actually came, and were asked to report the total number of stimuli they received. So the factor of attention might be playing a role for these results. And it all makes sense when we look at the results obtained for the nociceptive passive condition, where the responses obtained over the temporal regions for the pre-stimulus interval disappeared in the Gabor window showing the significant differences (Fig. 7.10). This shows that the factor of attention is affecting the results for the nociceptive stimulation in the way the differences between the types of stimuli (deviant and standard) are presented and reflected on the scalp. This result coincides with the ones found in [21] where different results were obtained for different conditions depending on the level of alertness.

As we mentioned in the results section, we obtained the same result for the somatosensory condition, where we did have significant values during the pre-stimulus interval over the temporal regions when we compared the types of stimuli but only during the active condition, and such results were not presented in the results for the passive condition. So once again the factor of attention is driving the results.

However during the somatosensory condition the main differences between the standard and deviant stimuli were found around the 30 Hz with a latency of 22ms before the stimulus. It is quite interesting the fact that the latency was almost the same as the one found for the nociceptive condition but the frequency was diminished in 10Hz, suggesting that pain signals are activating

higher frequencies on their way up to the cortex and that is why we decided to make a comparison between nociceptive and non-nociceptive condition in section 7.5.

For this comparison between the nociceptive and somatosensory condition, over the central region the Gabor windows were widely different for both the standard and deviant stimulus. The difference were found from 10Hz to 60Hz and latency from 30ms before the stimulus to 96ms after the stimulus for the deviant stimulus, and from 8Hz to 62 Hz and latency from 46ms before the stimulus to 70ms after the stimulus for the standard stimulus. This time the differences cover a wide range in both the frequencies and latency which suggest a big gap difference in how the information is processed for the nociceptive stimulus compared to a somatosensory (non-nociceptive) stimulus.

The evoked potentials were consistent with these results, and in both the deviant stimulus and standard stimulus the amplitude was larger for the nociceptive evoked potentials during the latencies representing more difference in the Gabor windows. Larger amplitude in the signal is directly resulted in larger energy which would imply that the transmission of nociceptive signals in the nervous system somehow uses more energy than that needed to transmit a non-nociceptive signal.

Moreover, even though the latencies and frequencies activated in the Gabor windows slightly vary, this result was consistent over the three regions of interest, which enhances the fact that "pain" signals are reflected in the scalp as electric signals with more energy compared to those non-nociceptive signals.

Well now, what about the nociceptive passive vs. the somatosensory passive comparison?. The results were once again consistent with the fact that the signals related to pain represent more energy. However the range of the frequencies that represent a significant difference in the Gabor windows is not as large as the ones found in the last comparison (nociceptive active vs. the somatosensory active) except for the central region.

In the central region the frequencies representing significant difference are in the range from 5Hz to 62Hz for the deviant stimulus and from 3Hz to 63Hz for the standard stimulus (Fig. 7.26).For the temporal regions the range of frequencies representing significant difference in the Gabor windows was not as large. Nevertheless the energy for such frequencies during the significant latencies was larger for the nociceptive evoked potentials as we can see in the evoked potentials.

9

Conclusions

Performing a time-frequency analysis using the wavelet transform gave us reliable information that allowed us to recognized features over the evoked potentials, such as frequencies that were activated as well as the latencies in which the different evoked potentials differed from each other.

We obtained significant results for the Gabor windows over the temporal regions for the nociceptive active condition, showing differences between the standard and deviant stimuli for frequencies between 38Hz and 40Hz at a latency of 24ms before the stimulus. On the other hand, for the nociceptive passive condition we obtained no significant differences between standard and deviant stimuli in the Gabor windows. This drove us to think that the factor of attention played a role in the sense that it provoked different evoked potentials when the participants were focusing on the stimuli, and thus the standard stimulus and deviant stimulus were different for the active condition.

Same type of result was obtained for the somatosensory active condition and somatosensory passive condition. However, in this case the Gabor window comparing the standard and deviant stimuli also showed differences over the central region. Another important difference is the frequency where we found significant values on the Gabor window, for the nociceptive active condition it was around 40Hz but for the somatosensory active condition it was 30Hz. Thus we can say the pain signals are reflected in the scalp at higher frequencies.

Not only the frequency was different when comparing the nociceptive stimulus with the deviant stimulus. It was a constant in the results that the energy found in the signals evoked by nociceptive stimulation is larger to those evoked by somatosensory non-nociceptive signals.

10

Acknowledgement

Special thanks to Li Hu, Chen Zhao, Hong Li, and Elia Valentini for having shared the EEG database which made possible this work come true.

Bibliography

[1] Li Hu and Zhiguo Zhang. Detection of pain from nociceptive laser-evoked potentials using single-trial analysis and pattern recognition. *2012 IEEE International Conference*, pages 67–71, August 2012.

[2] Brayan Arias Martinez. Diseño y desarrollo de un sistema para la adquisición y procesamiento de una señal eeg para la visualizacion de la onda p300 a partir de potenciales evocados : aplicación en tareas cognitivas de reconocimiento del nombre de pila. Master's thesis, Universidad de los Andes, 2009.

[3] Bao-Ming Li Hu Lu and Hui Wei. A small-world of neuronal functional network from multi-electrode recordings during a working memory task. *Neural Networks (IJCNN), The 2012 International Joint Conference*, 2012.

[4] Carlos Alfonso Bayter Rey. Evaluacion de la sonorización de senales de eeg en la anticipacion de crisis de epilepsia. Master's thesis, Universidad de los Andes, 2011.

[5] Catalina Alvarado Rojas. Estudio de la factibilidad del uso de predictores basados en análisis en tiempo-frecuencia de señales de electroencefalografía (eeg) para la deteccion temprana de crisis epilecticas. Master's thesis, Universidad de los Andes, 2007.

[6] P. Panavaranan and Y. Wongsawat. Eeg-based pain estimation via fuzzy logic and polynomial kernel support vector machine. *Biomedical Engineering International Conference*, 2013.

[7] Jon D. Levine David B. Reichling, Paul G. Green. The fundamental unit of pain is the cell, May 2013. ISSN 0304-3959.

[8] David Fitzpatrick Anthony-Samuel LaMantia James O. McNamara Dale Purves, George J. Augustine and Leonard E. White. *Neuroscience*. Sinauer Associates Inc., 4th edition, 2007.

[9] David Fitzpatrick William C. Hall Anthony-Samuel LaMantia James O. McNamara McNamara Dale Purves, George J. Augustine and S. Mark Williams. *Neuroscience*. Sinauer Associates Inc., 3rd edition, 2007.

[10] Luigi Benedicenti Raman Paranjape, J. Mahovsky and Z. Koles. The electroencephalogram as a biometric. *Electrical and Computer Engineering, 2001,Canadian Conference on*, 2:1363 – 1366, 2001.

[11] D. J. McFarland G. Pfurtscheller J. R. Wolpaw, N. Birbaumer and T. M. Vaughan. Brain-computer interfaces for communication and control. *Clinical Neurophysiology*, 113(6):767âĂŞ791, 2002.

[12] S. Kumar Singh Y. Narain Singh and A. Kumar Ray. Bioelectrical signals as emerging biometrics: Issues and challenges. In *International Scholarly Research Notices*, pages 1–13. 2012.

[13] L. Sörnmo and P. Laguna. *Bioelectrical Signal Processing in Cardiac and Neurological Applications,*. Elsevier.

[14] Trans Cranial Technologies ltd. 10/20 system positioning. 2012. Hong Kong.

[15] A. H. and E. O. Independent component analysis: algorithms and applications. Elsevier, 2000.

[16] T. Sejnowski A. Delorme, T. P. Jung and S. Makeig. Improved rejection of artifacts from eeg data using,. *Neuroimage*, 34:1443–1449, 2007.

[17] S. Mozaffar and D. W. Petr. Artifact extraction from eeg data using independent component analysis. Technical report, The University of Kansas for Research, 2335 Irving Hill Road, 2002.

[18] S. Chartier D. Langlois and D. Gosselin. An introduction to independent component analysis. *Quantitative Methods for Psychology*, 6:31–38, 2010.

[19] Charles K. Chui. *Wavelet Analysis and its Applications*. Academic Press, 1992.

[20] Jian-Jiun Ding Ke-Jie Liao. An indtroduction to time-frequency analysis. Technical report, National Taiwan University.

[21] Hong Li Elia Valentini Li Hu, Chen Zhao. Mismatch responses evoked by nociceptive stimuli. *Psychophysiological*, 50:158–173, February 2013.

[22] A. Delorme and S. Makeig. Eeglab: an open source toolbox for analysis of single-trial eeg. *Journal of Neuroscience Methods*, 134:9–21, 2004.

[23] J. Onton. Artifact rejection and running ica, 2010, Retrieved April 2015. http://esciedu.nctu.edu.tw/eeglab_workshop/ch/doc/2_ArtRej_RunningICA.pdf.

[24] A. Delorme and S. Makeig. Eeglab wiki, 2014, Retrieved April 2015,. http://sccn.ucsd.edu/wiki/Chapter_09:_Decomposing_Data_Using_ICA.

[25] Cognition Medical Research Council and Brain Sciences Unit. Introduction to eeg and meg, 2013, Retrieved April 2015. http://imaging.mrc-cbu.cam.ac.uk/meg/IntroEEGMEG.